The Aerosol Collector Pyrolyser (ACP) Experiment for Huygens

G. Israel,[*][1] H. Niemann,[3] F. Raulin,[4] W. Riedler,[5] S. Atreya,[6] S. Bauer,[7] M. Cabane,[3] E. Chassefière,[3] A. Hauchecorne,[3] T. Owen,[8] C. Sablé,[9] R. Samuelson,[3] J. P. Torre,[2] C. Vidal-Madjar,[10] J. F. Brun,[**][2] D. Coscia,[2] R. Ly,[2] M. Tintignac,[2] M. Steller,[5] C. Gelas,[11] E. Condé[11] & P. Millan[9]

[1]*Service d'Aéronomie du CNRS, F-91371 Verrières le Buisson, France*
   E-mail: guy.israel@aerov.jussieu.fr   Fax: +33 1 69 20 29 99
[2]*Service d'Aéronomie du CNRS, F-91371 Verrières le Buisson, France*
[3]*NASA Goddard Space Flight Center, Greenbelt, MD 20771, USA*
[4]*Laboratoire Interuniversitaire Systèmes Atmosphériques (LISA), Universités Paris VII et Paris XII, F-94010 Créteil, France*
[5]*Space Research Institute, A-8010 Graz, Austria*
[6]*University of Michigan, Ann Arbor, MI 48109, USA*
[7]*Institüt für Meteorologie und Geophysik, A-8010 Graz, Austria*
[8]*University of Hawaii, Honolulu, HI 96822, USA*
[9]*Office National d'Etudes et de Recherches Aerospatiales, CERT, F-31055 Toulouse, France*
[10]*Laboratoire de Physico-Chimie des Biopolymères, CNRS, F-94320 Thiais, France*
[11]*CNES, F-31401 Toulouse, France*
*ACP Principal Investigator   **ACP Project Manager

1. Introduction

The Service d'Aéronomie du Centre National de la Recherche Scientifique (SA/CNRS) is the Principal Investigator institute for the Aerosol Collector Pyrolyser (ACP) experiment aboard Huygens. As such, it has overall responsibility for the complete instrument.

ACP's main objective is the chemical analysis of the aerosols in Titan's atmosphere. For this purpose, it will sample the aerosols during descent and prepare the collected matter (by evaporation, pyrolysis and gas products transfer) for analysis by the Huygens Gas Chromatograph Mass Spectrometer (GCMS). ACP's products transfer line (PTL) directly interfaces with an ACP-devoted GCMS feed tube. GCMS is used by ACP for about 20% of its operating time, based on a cooperative agreement between SA/CNRS (ACP) and NASA Goddard (GCMS).

ACP is also the result of a close scientific collaboration between France (SA/CNRS) and Austria (Space Research Institute, Graz). Austria's contribution involves the electronic segment: Flight Model hardware and software; electrical ground support equipment (EGSE). SA/CNRS is also supported by CNES in Toulouse, which had the technical responsibility for the fabrication and qualification of ACP's mechanical and pneumatic components.

For the operational validation tests and calibration, SA/CNRS was assisted by the co-investigator institutes, principally: the Laboratory for Planetary Atmospheres at NASA Goddard, the Laboratoire Interuniversitaire Systèmes Atmosphériques (LISA) at Créteil and ONERA/CERT at Toulouse.

For Europe's contribution to ACP, the funding resources are principally CNES and CNRS in France, and SRI and the Ministry for Research in Austria. The prime industrial contractors were SEP (Melun Villaroche, France), The Joanneum Research Institute (Graz, Austria) and Schrack Aerospace (Vienna, Austria).

2. ACP Scientific Objectives

Our approach for selecting ACP's scientific objectives was to rely on the micro-physics models and on the results of specific laboratory studies.

Two methods of producing Titan-like aerosols in the laboratory have been investigated. The first involves identifying these aerosols within the complex organic material that is often observed in the laboratory from simulating the photolytic and radiolytic processes expected in Titan's atmosphere. This material roughly corresponds to what Sagan's group labels 'tholins'. The second route for producing the yellowish aerosols that might correspond to those of Titan is by polymerising organic molecules using UV. The best candidate is C_2H_2, which polymerises more easily than C_2H_4 or HCN.

These polymers are expected to form the aggregates that are needed to reconcile polarimetric and photometric results (West & Smith, 1991; Cabane et al., 1993; Rannou et al., 1994). The optical properties of tholins and C_2H_2 polymers are in agreement with Voyager's observations. The chemical processes leading to these different particle types are not expected to occur in the same altitude ranges, owing to the diversity of the possible energy sources and their related vertical distribution. The polymerisation of C_2H_2 through the action of solar UV photons is expected, from current modelling, to yield $C_{2n}H_2$ at altitudes greater than ≈ 500 km. The synthesis, in large amounts, of polymers of the form $(C_2H_2)_n$ in the lower stratosphere may be considered as rather unlikely, but depends on how the acetylene polymerises long-ward of 190 nm (Chassefière & Cabane, 1995). The formation of C-H-N tholin oligomers by the action of suprathermal Saturn plasma electrons, around 900-1000 km, or of energetic radiation belt particles at 350-400 km altitude, is shown to be the most plausible mechanism for explaining the haze's formation. Laboratory experiments providing the best reproduction of Titan's stratospheric conditions are needed to test, for example, the gas phase behaviour of tholin aerosols, and the optical properties of tholin or poly-C_2H_2 particles.

In the low stratosphere, aerosol particles settling down from the upper levels may act as condensation nuclei. Below ≈ 80 km, this should lead to the deposition of thin layers (< 0.01 μm) of condensed gases (e.g. HC_3N, HCN, C_4H_{10}) on the sub-μm particles. This first stage is followed by a more consistent increase in the particle size, up to a few μm, where the condensation of CO_2, C_3H_8, C_2H_2 and C_3H_6 occurs, between 67 km and 63 km (Frère et al., 1990). The main condensation processes occur near the tropopause, with the condensation of C_2H_6 below 62 km, and in the troposphere, where CH_4 and N_2 condense on the resulting particle, which may yield cloud droplets (≈ 100 μm, see Toon et al., 1992). Another source of condensation nuclei may be the particles produced directly at these altitudes by the radiolysis of organic gases. The energy deposition of cosmic rays peaks near 60 km and, as on Earth, lightning may exist in the low troposphere.

Tholins obtained from the sparking of He-CH_4 and N_2-CH_4 mixtures have been studied with the ACP experiment in mind (Israel et al., 1991; see also Raulin et al., 1992). The pyrolysis gas chromatography (Py-GC) of tholins produced at 77 K shows them to include saturated and unsaturated carbon chains in their structure; N-containing groups appear in the case of N_2-CH_4 sparking. The thermal desorption profile of these tholins clearly showed two peaks, the first corresponding to the distillation of condensed species, the second to the pyrolysis. The mass spectrometer (MS) study of the evaporated oligomers and pyrolysis products showed that a wide range of alkylated aromatic compounds evolved from the sample, which indicates that such solids contain a 3-D polymer with a high degree of branching.

In other work (Ehrenfreund et al., 1995), the main peaks related to N-compounds observed in the GCMS are HCN, CH_3CN, C_2H_5CN and longer chain nitriles. Only the saturated hydrocarbons are observed. The study of the evolution with temperature shows that HCN is a dissociation product during the whole Py-GC analysis process,

which may imply that the nitriles can form thermostable structures in the tholins.

From the above and from previous assessment, two classes of scientific objectives have been adopted:

Primary objectives, can be satisfied from measurements made during Probe entry by ACP coupled with GCMS:

1. Determine the chemical makeup of the photochemical aerosol, i.e. infer the relative numbers of constituent molecules (C, H, N, O) composing the aerosol.
2. Obtain the relative abundances of condensed organics (e.g. C_2H_2, C_2H_6, HC_3N, HCN) in a column average throughout the stratosphere. Compare with the abundance of constituent molecules in the aerosol nucleation sites.
3. Obtain the relative abundances of condensed organics (principally CH_4, plus organics listed above) in a column averaged over the upper troposphere. Compare with the abundances of constituent molecules in the aerosol nucleation sites.

Secondary objectives of fundamental interest can also be satisfied with the aid of additional information acquired by other Probe instruments (mainly the Descent Imager/Spectral Radiometer):

4. Obtain absolute abundance for all condensed species, averaged over the stratosphere and upper troposphere respectively.
5. Determine the mean sizes of aerosol nucleation sites averaged over the stratosphere, and compare with those in the upper troposphere.
6. Detection of non-condensable species, such as CO, eventually trapped in aerosols.

Fig. 1 provides an overview of ACP. The gas products transferred from ACP are analysed by GCMS (see the GCMS paper in this volume).
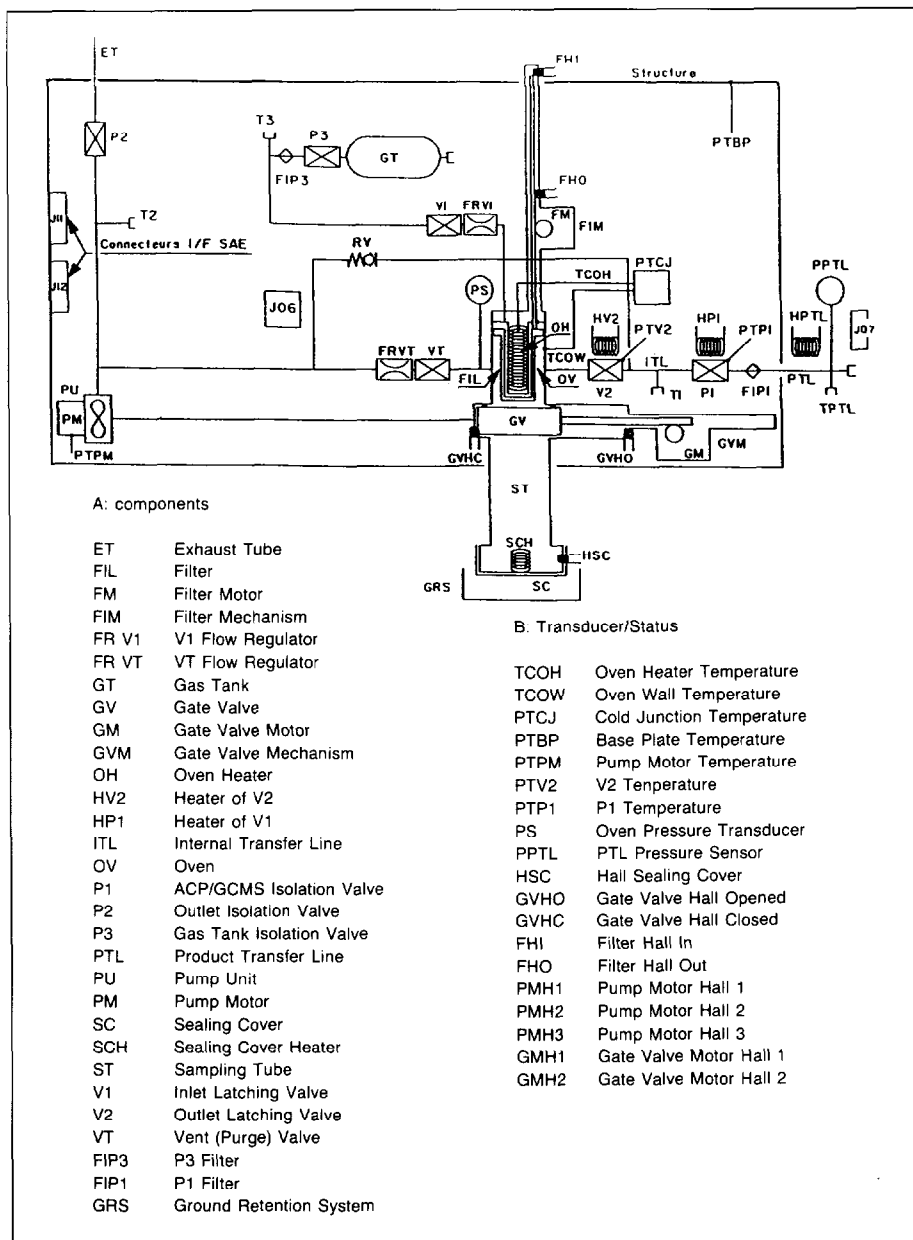
3. Functional Description

A sampling system is required for sampling the aerosols in the 135-32 km and 22-17 km altitude regions of Titan's atmosphere. These altitude ranges refer to the Probe's nominal descent profile (Lebreton & Matson, 1997).

The sampling system requires an inlet (sampling) tube (ST) extending beyond the boundary layer (estimated to be few mm thick): the end protrudes 28 mm from the Probe's fore dome. During sampling, the collecting target's temperature must be as close as possible to that of Titan's atmosphere in order to help retain the more volatile aerosol and cloud particle components. The target is a filter (FIL), made in stainless steel (Beckaert ST10), that can be moved along the inlet tube. When the filter is in its sampling position, its front face extends a few mm beyond the inlet tube. This increases aerosol collection by direct impaction at high altitude, where the pump does not operate (see below).

Before descent, the filter is held in its storage position inside the oven (OV). During descent, a mechanism (FIM) can move the filter to its sampling position and return it into the oven.

The oven is a pyrolysis furnace where a heating element (OH) can heat the filter and hence the sampled aerosols to 250°C or 600°C. A motorised gate valve (GV) can be activated to close the furnace after filter retraction. Three normally-closed monostable valves (V1, V2, VT) are mounted on the oven's body. V1 supplies a labelled gas ($^{15}N_2$) to carry the gas sample from the oven to the transfer lines through V2. The venting valve VT allows the oven's gas content to be vented to Titan's atmosphere. VT is also usually activated during certain sequences for purging operations or under pressure control before transfers (see below). Also, VT can be opened at any time during

Fig. 1. Aerosols Collector Pyrolyser (ACP) schematic.

A: components

ET	Exhaust Tube
FIL	Filter
FM	Filter Motor
FIM	Filter Mechanism
FR V1	V1 Flow Regulator
FR VT	VT Flow Regulator
GT	Gas Tank
GV	Gate Valve
GM	Gate Valve Motor
GVM	Gate Valve Mechanism
OH	Oven Heater
HV2	Heater of V2
HP1	Heater of V1
ITL	Internal Transfer Line
OV	Oven
P1	ACP/GCMS Isolation Valve
P2	Outlet Isolation Valve
P3	Gas Tank Isolation Valve
PTL	Product Transfer Line
PU	Pump Unit
PM	Pump Motor
SC	Sealing Cover
SCH	Sealing Cover Heater
ST	Sampling Tube
V1	Inlet Latching Valve
V2	Outlet Latching Valve
VT	Vent (Purge) Valve
FIP3	P3 Filter
FIP1	P1 Filter
GRS	Ground Retention System

B. Transducer/Status

TCOH	Oven Heater Temperature
TCOW	Oven Wall Temperature
PTCJ	Cold Junction Temperature
PTBP	Base Plate Temperature
PTPM	Pump Motor Temperature
PTV2	V2 Tenperature
PTP1	P1 Temperature
PS	Oven Pressure Transducer
PPTL	PTL Pressure Sensor
HSC	Hall Sealing Cover
GVHO	Gate Valve Hall Opened
GVHC	Gate Valve Hall Closed
FHI	Filter Hall In
FHO	Filter Hall Out
PMH1	Pump Motor Hall 1
PMH2	Pump Motor Hall 2
PMH3	Pump Motor Hall 3
GMH1	Gate Valve Motor Hall 1
GMH2	Gate Valve Motor Hall 2

descent as a safety measure if the oven pressure rises above 3.2 bar; it closes when the pressure falls to 2.7 bar.

A drag fan kinetic pump (PU) ensures the flow of Titan's atmosphere through the filter, at a rate depending on altitude. An exhaust tube (ET), with a one-shot isolation valve (P2), allows the gas to be vented externally. The gas flow, on reaching the level of the GV, follows a path perpendicular to the oven/GV assembly. The result is that the circulation is independent of the GV status (closed or open). When it is switched off, PU acts as a flow-blocking device. The pressurisation system for storing N₂ gas and controlling its flow to the oven begins with a gas tank (GT) at 40 bar. Oven filling is controlled by a pressure transducer (PS) associated with valve V1 (see Section 5). A relief valve (RV, set at 4.1 bar) in the internal gas transfer line protects GCMS against accidental ACP overpressure.

The whole internal circuit is pressurised during ground operations and the early part of the flight to Saturn. After the Jupiter flyby, about 3 years after launch, ACP's internal circuit is evacuated by opening P2. In addition, valves V1, V2 and VT are

opened briefly during each cruise phase checkout. The gate valve mechanism (GVM) is locked during launch, and unlocked shortly after. It must be locked again for a short time before Probe entry; this is done during the last cruise checkout sequence. The inlet tube end is closed by a sealing cover (SC), which will be opened at the beginning of descent. A connecting tube (Product Transfer Line, PTL) between ACP and GCMS transfers the pyrolysis products. Valve P1 isolates the ACP internal circuit from the product transfer lines. This one-shot isolation valve is opened at the beginning of descent ($T_0 + 2$ min) for an initial venting of the internal (ITL) and the external (PTL) exit transfer lines. The IVA one-shot valve (see Fig. 3 and the GCMS paper in this volume) isolates the PTL at its GCMS extremity. The T1, T2 and T3 special ports are for ground tests. The V2 and VT electrovalves, P1 and PTL can be heated by special heaters (HV1 for V1, HV2 for V2, HVT for VT, HP1 for P1 and HPTL for PTL). In addition, heater HV1 (not shown in Fig. 1) is controlled by a thermostat, activated when the temperature falls below -5°C. This prevents leakage caused by Titan's low temperatures.

4. Measurement Strategy

The operations sequences result from the following requirements:

1. Determining the compositions of the particle cores (non-volatile and volatile components) is conducted mainly in the low stratosphere and down to the tropopause (above 30 km). In the higher part of the descent (above 80 km), it is expected that aerosols will be obtained by direct impaction on the filter. Below 80 km, where the pump becomes effective, the samples are obtained by filtration.

2. The second sample must be collected within the troposphere above the deep methane clouds (20 km).

3. Owing to mass constraints, the instrument is equipped with a single collector that must be used again after cleaning the oven, filter and product transfer lines.

4. The samples are analysed by using GCMS for a fixed portion of its life (approximately 20 min), knowing that this instrument must make at least one direct chromatographic analysis of the atmosphere's composition before surface impact.

In addition, because of the very short descent profile (120 min minimum), it was decided to make three transfers for each sample, each transfer using the direct MS mode (see the GCMS paper in this volume). These will use, in turn, the oven at ambient temperature, 250°C and 600°C. A complete GCMS analysis, requiring about 10 min, is provided only for the first sample's pyrolysis sequence (transfer after 600°C heating). These pyrolysis products have to wait until GCMS has analysed the contents of the two gas enrichment cells that were sampled in the upper atmosphere. This implies that the use of the three gas chromatograph columns for analysing ACP aerosol pyrolysis products obtained at 600°C occurs at $T_0 + 73$ min (nominal altitude 25 km).

5. Operation Sequences during Descent

A detailed timeline has been formulated to mesh with GCMS' own (Fig. 2). It is based on the following sequences that ACP must operate during the descent phase.

Sequence 1 Initial venting and preparation for the first sampling operation between ACP initialisation (at $T_0 + 1$ min 40 s) and the filter in its sampling position (at $T_0 + 6$ min 45 s, nominal altitude 130 km).

Sequence 2 First sampling in the low stratosphere. This period ends when the filter is retracted into the oven (GV locked) at $T_0 + 60$ min 00 s (nominal altitude 32 km).

Sequence 3 Heating the filter (ambient, 250°C, 600°C) and gas product transfers to GCMS at T_0+74 min 00 s (nominal altitude 24 km).

Sequence 4 Oven and transfer lines cleaning, and preparation for the second sampling operation with the filter in its sampling position at T_0+77 min 00 s (nominal altitude 22 km).

Sequence 5 Second sampling in the upper troposphere. This period ends when the filter is retracted into the closed oven, at T_0+89 min 00 s (nominal altitude 17 km).

Sequence 6 Heating the filter (ambient, 250°C, 600°C) and gas product transfers to GCMS ends at T_0+108 min 00 s (nominal altitude 9 km).

During sequence 1, after the high entry velocity has been reduced and the Probe's protective front shield has been jettisoned — eliminating the risk of contamination from the front shield — the following operations begin at T_0+1 min 40 s. P3 is opened, and flushing and venting the internal circuit begins by filling the circuit with N_2 through V1 and V2 down to P1 (GV is closed). Venting is obtained by opening VT. The whole process is repeated after opening valve P1. The mechanism for ejecting the sealing cover (SC) is then activated, and in-flight calibration of the oven pressure sensor (PS) is performed to compensate for any offset accumulated during cruise. GV is then opened and the filter is moved into its sampling position.

Sequence 2 begins immediately, with its two sampling modes. The first leaves the pump unit inactive (until approximately T_0+23 min 30 s), so that sampling is by direct impaction. The second turns the pump unit, so that sampling is mainly by filtration. Once the pump is switched off, the filter is retracted and the oven gate is closed. Retraction and oven closing is accomplished in only 13 s in order to avoid any evaporation of certain condensates in the aerosols. The whole of sequence 2 takes about 55 min.

Sequence 3 deals with:

1. the preparation of aerosols for producing evaporates and pyrolysis products;
2. the transfer of gas products to the ACP line (feed tube to GCMS);
3. the analysis either by the sole direct MS mode or the complete mode (GCMS + direct MS; see the GCMS paper in this volume).
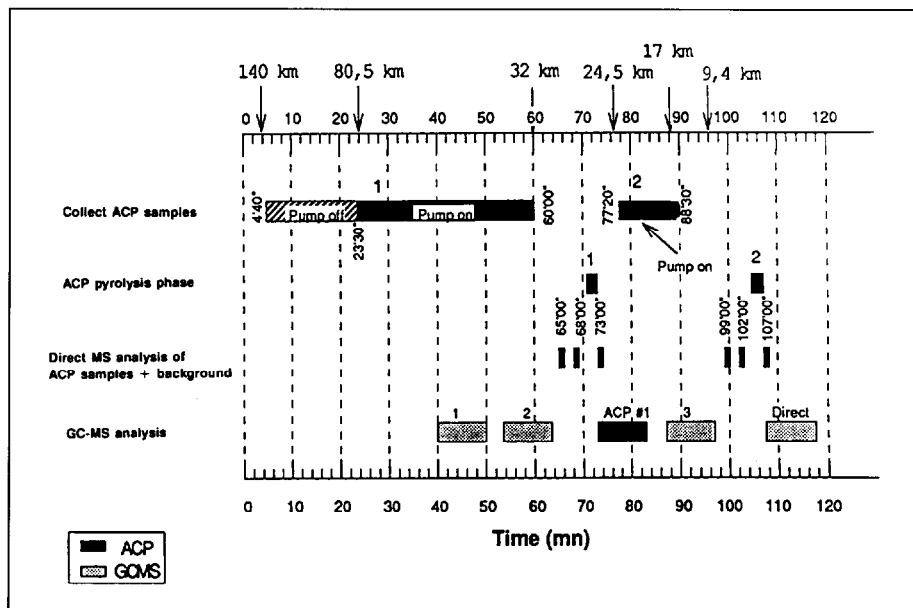

Fig. 2. GCMS sequence of operations for ACP gas products analysis.

The programme for aerosol preparation and transfer consists of three phases:

Phase (a) transfer of the gas products obtained while the filter is in the unheated oven. At the time of transfer, the filter has considerably warmed since oven closing, and the temperature gradient is sufficient to produce some evaporates.

Phase (b) transfer of gas products obtained after heating the filter to $T_f = 250°C$. In order to avoid excessive pressure in the oven and thence in the ACP feed tube in GCMS, the oven is linked before heating to the atmosphere by briefly opening VT. In addition, to avoid condensations of gas samples, transfer lines ITL and PTL (valves and tubing) are heated as much as possible within the constraint of the allocated power; 90°C is the objective. During the transfer time (~ 1 min), the filter temperature is maintained by holding T_f at 250°C.

Phase (c) transfer of the gas products obtained after heating the filter to 600°C. This pyrolysis phase is also preceded by briefly opening VT to reduce pressure to atmospheric. During transfer, the valves and tubes are heated within the power constraint as in phase (b); the goal is again 90°C.

Fig. 3 is a schematic of the ACP-GCMS interface. In order to transfer the gas samples with minimal dilution from the effluent gas ($^{15}N_2$), each injection into GCMS is done by pressurising the oven to 2.5 bar with N_2 (V1 controlled, V2 closed) and then rapidly depressurising it (fast actuation of V2 and VAB). The estimated mass flow rate at injection is 3-9 mg/s at 2 bar N_2.

A description of the transfer cycle is given by Fig. 4. The same cycle is used for each analysis that occurs after phase (a), (b) and (c). As there are two sampling operations (one high altitude, one low altitude), the complete ACP programme equates to six transfer cycles.

Each transfer cycle comprises two sub-cycles. The 'scientific sub-cycle' is devoted to analysing the oven contents by a series of six injections (V1 closed) of 0.875 s (V2 and VAB open) each, each followed by an MS analysis period of 4.750 s. This period for MS analysis is longer than the time required by GCMS for a full mass scan. As shown in Fig. 4, after completion of the sixth MS analysis, VT and VAA are opened (VL4 is closed) for 5 s to evacuate any residual traces of pyrolysis products in the sampled volume. A second sub-cycle follows, devoted to a background analysis. Two 0.875 s injections are each followed by an MS analysis of 4.750 s. A second 5 s vent (VAA and VT open) completes the transfer cycle.

The oven pressure must be controlled during each transfer for a correct GCMS analysis. An optimal interface requires that the pressure in the GCMS feed tube is maintained above 1.9 bar. Also, efficient sample transfer requires pre-injection pressurisation of the oven to 2.5 bar. During the pressurisation period (625 ms) a control loop uses the oven's pressure sensor to stay within the 2.5 bar limit (by closing
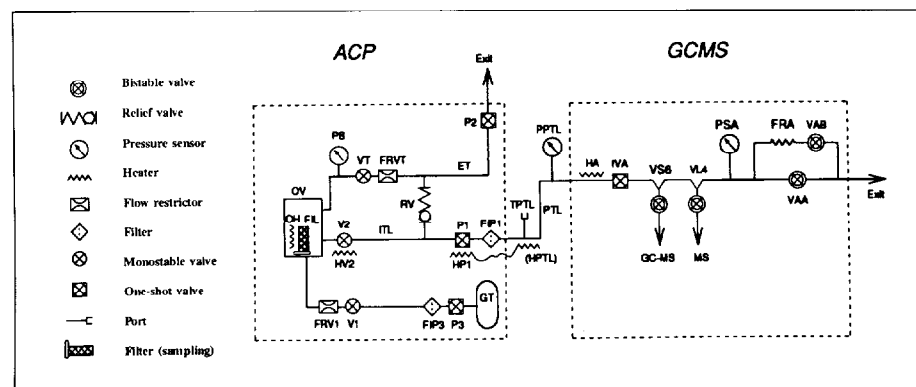

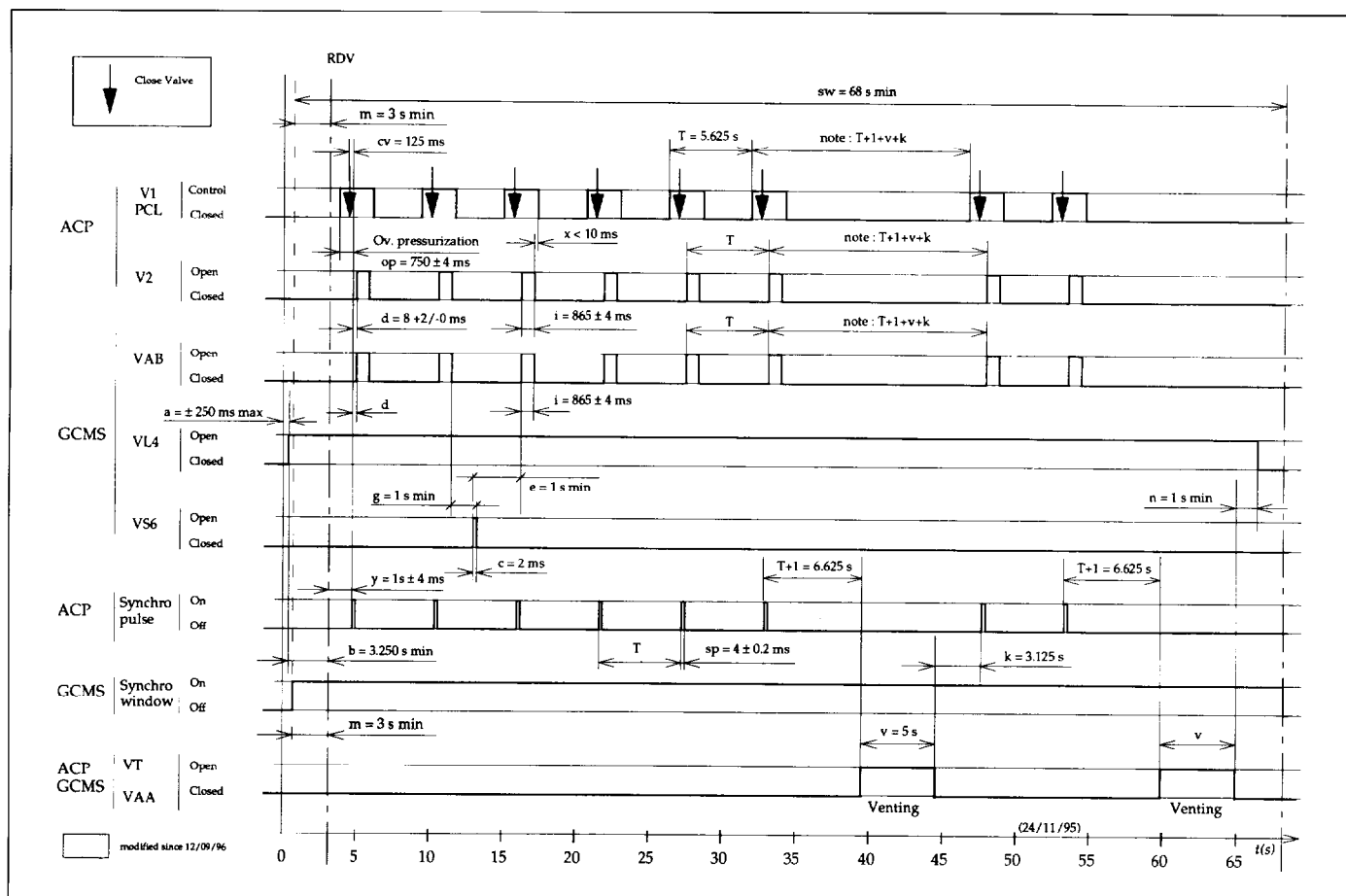Fig. 3. Schematic of the ACP-GCMS transfer interface.

Fig. 4. ACP-GCMS transfer cycle.

V1 if needed). During injection, the control loop ensures a minimum 1.9 bar in the oven by opening V1 if necessary. (Note that V1 is closed by the software as part of the transfer cycle in any case at the end of the 625 ms pressurisation period; see Fig. 4).

Furthermore, because of the unknown aerosol load collected on the filter, we have to accommodate any unforeseen increase in oven pressure after heating. The oven pressure is therefore checked before each transfer cycle. If it is above the nominal 2.7 bar, VT is opened until this value is reached.

Owing to the peak power limit imposed by the Probe system (83 W on the ML3 main power line, see Section 9.1), there is a conflict between heating the oven and the transfer lines during the transfer cycle. It was thus imperative that a temperature control priority be selected by the software. The result is that heating the oven and holding it constant during the transfer of gas products to GCMS has first priority. Second priority is given to heating VT, P1 and PTL. In addition, during the preparation phase sub-sequence before oven heating, the temperature control loop of the transfer lines activates their heating for 1-2 min at 120°C.

For sequence 4, before the second sampling stage, the filter, oven walls and transfer lines must be well cleaned. The oven and filter are cleaned, first, by extending oven heating by 1 min in order to complete filter outgassing (filter temperature is 600°C at the end of sequence 3's last transfer). Immediately after, the oven is filled to 2.5 bar within 3 s by activating the oven's pressure control loop to open V1. Then, the oven is vented by opening VT for about 6 s, reducing the pressure down to ambient atmospheric. Cleaning the transfer lines downstream of V2 is achieved first by switching on heaters HV2 and HP1 (plus PTL), set at the maximum 120°C, for 90 s. Then, a fill-vent phase is started for the oven and transfer lines by:

1. switching on the oven's pressure control loop (filled at a maximum 2.7 bar) while valve V2 is opened for approximately 3 s;
2. venting the two circuits when reducing the internal pressure to the external level at the two ends. The oven is vented by opening VT (6 s), while the transfer lines downstream of V2 are vented through GCMS by opening VAA (few seconds).

This fill-vent operation is repeated once. There is no background analysis from the MS in order not to contaminate the GCMS instrument unnecessarily. At the end of sequence 4, ACP is ready for a second sampling sequence.

For sequence 5, sampling is performed by filtration in the cloud region. The altitude range is fixed by the time at which the pyrolysis products analyses must be finished so that GCMS is freed for direct GCMS analysis of the atmosphere (see Section 4). It means that the second sampling phase, which starts T_o+77 min (nominal descent profile, 22 km) must be finished at T_o+88 min 30 s (17 km nominal descent profile). Then, after about 11 min of sampling, the filter is moved back into the oven, which is closed for preparation and analysis.

Before dealing with the next sequence, there is a standby period of 9 min in order to wait for GCMS as it completes its analysis of sample cell number 3 (see the GCMS paper in this volume).

Sequence 6 is a copy of sequence 3 but during phase (c) there is no time left for GCMS to analyse the pyrolysis products through the columns - only the MS mode is used. Purging and background analysis are, as in sequence 3, performed after phase (a) and again after phase (b/c). At the end of the transfer (phase c) of the products to GCMS $(T_o+108$ min), ACP is prepared for being turned off until T_o+110 km (8 km nominal altitude).

6. Mechanical Configuration

The instrument housing is made of aluminium alloy and consists of a single unit mounted on the lower part of the experiment platform. The rectangular box carries six attachment lugs on its base. The electronics system (ACPE) has its own structure attached at six points on one side of the instrument's main body, in which the mechanical and pneumatic subsystem is located. Fig. 5 shows the electronics box attached, along with the sampling tube and its sealing cover.

ACP's maximum dimensions are 220x200x206 (H) mm. In addition to the inlet and exhaust tubes, and to the GCMS product transfer tube, there is an extension accommodating movement of the filter mechanism's rack (see Section 7). ACP's total mass is 6.7 kg (including 5% margin), shared between 4.5 kg for the mechanical box and 2.2 kg for the electronics box.

The aerosols sampling inlet tube extends downwards to penetrate the Probe's fore dome. To provide efficient evacuation of Titan's atmospheric gas after sampling and filtering, the exhaust tube exits upwards, passing through the experiment platform and the top platform. By siting ACP close to GCMS, the inlet tube is close to the Probe's axis and PTL is as short as possible. A very strict procedure for limiting chemical contamination was followed during instrument fabrication. The objective values specified for the internal circuit of the gas transfer subsystem are <50 ppb for the organic compounds expected during aerosol chemical analysis and for gases such as CO_2, CO and H_2O. The internal surfaces of all the transfer tubes have been passivated ('silanised'). A cleanliness plan was followed first at the level of each equipment element and then
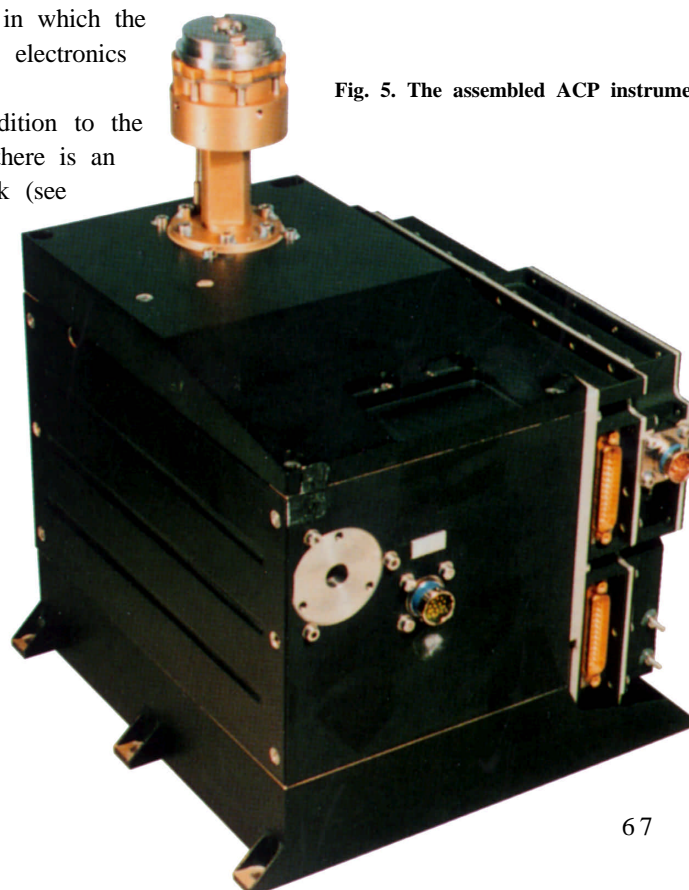

Fig. 5. The assembled ACP instrument.

at the instrument level. After assembly, the whole ACP was baked under vacuum for several days at 120°C. Also, organic materials were not used in the GV and filter mechanisms. Their bearings, in particular, are not lubricated.

In order to maintain the high cleanliness level during the instrument's ground storage and its first part of the cruise, ACP's internal gas circuit was filled to 2.5 bar with pure nitrogen. The internal circuit is hermetically closed off, by three sealing devices, at the level of the sampling and exhaust tubes and at the interface between the ACP housing and the PTL. The specified instrument overall helium leak rate of 10^{-7} mbar.litre.s^{-1} was found to be sufficient to hold the gas circuit pressurised for more than 4 years.

The two apertures leading to the atmosphere are sealed by specially-developed devices: the sealing cover (SC) for the sampling tube and the one-shot P2 valve for the exhaust tube. SC is screwed to the bottom of the sampling tube (ST); the tightness requirement is satisfied by a stainless steel O-ring gasket. SC's cap will be spring-ejected towards Titan at 11 m/s; the requirement was for 8.6 m/s in order to avoid back-collision with Huygens. The cap and spring, totalling 80 g, are held in position on SC's body by tin-silver solder. Ejection will be within 2 min of switching on the 53 W heater (SCH), as the alloy melts at about 150°C. Correct ejection is checked by a Hall effect sensor (HSC). The device's outline can be seen in Fig. 6, as described in Section 7. The P2 concept is identical: melting a brazing allows a spring to eject the sealing cover, freeing the outlet gas exhaust. The P1 one-shot isolation valve between the ACP housing and PTL (see below).

7. Integrated Mechanical System

Fig. 6 shows the oven and GV assembly, plus the mechanism that translates the filter through the sampling tube. In the configuration shown in 6a and 6b, SC is attached to ST, and the filter (carried along by a rack) is in its inner position.

ST is a 70 mm-long, 45 mm-outer diameter aluminium cylinder that protrudes from the Probe's fore dome to position the filter directly in the gas flow, beyond the boundary layer. ST's upper extremity is fixed to the GV, and the crushing of a metallic O-ring gasket provides a tight seal between the two devices. At the bottom of ST, a stainless steel gasket made of flat surfaces assembled into a bellows ensures a tight fit with the filter. The gas flow is thus forced to pass through the wire netting. While the filter is in its sampling position (Fig. 6c), the magnet at the end of the rack provides a 17 N thrust forcing the filter against the bellows. A layer of alodine 1200 was deposited on the tube to increase conductivity.

The filter is a mesh brazed at one end to a mounting ring that interfaces with the rack of the filter mechanism. The mesh is made of multiple layers of stainless steel fibres. The filter's bottom end is a mesh disc laser-brazed to the mesh cylinder. This disc faces directly into the path of the gas and aerosols during sampling. When SC has been ejected and the filter is in its sampling position, the filter's bottom end is 4 mm below the cone-shaped entrance, 28 mm from the external surface of the Probe's fore dome.

7.1 Oven design and gas transfer system

The oven is the core of the mechanisms assembly shown in Fig. 6. Its cylindrical main body forms a common piece with the GV main body. The oven contains the filter, which has a thimble-like shape (inner diameter 10 mm, height 28 mm, thickness 0.5 mm). The heating element, from Thermocoax, is a resistance heater protected by a stainless steel (316L) shield and rolled inside the inner filter volume. Two thermo-couples, one for the heating element and one for the inner surface of the oven body, are used for thermal control and monitoring.
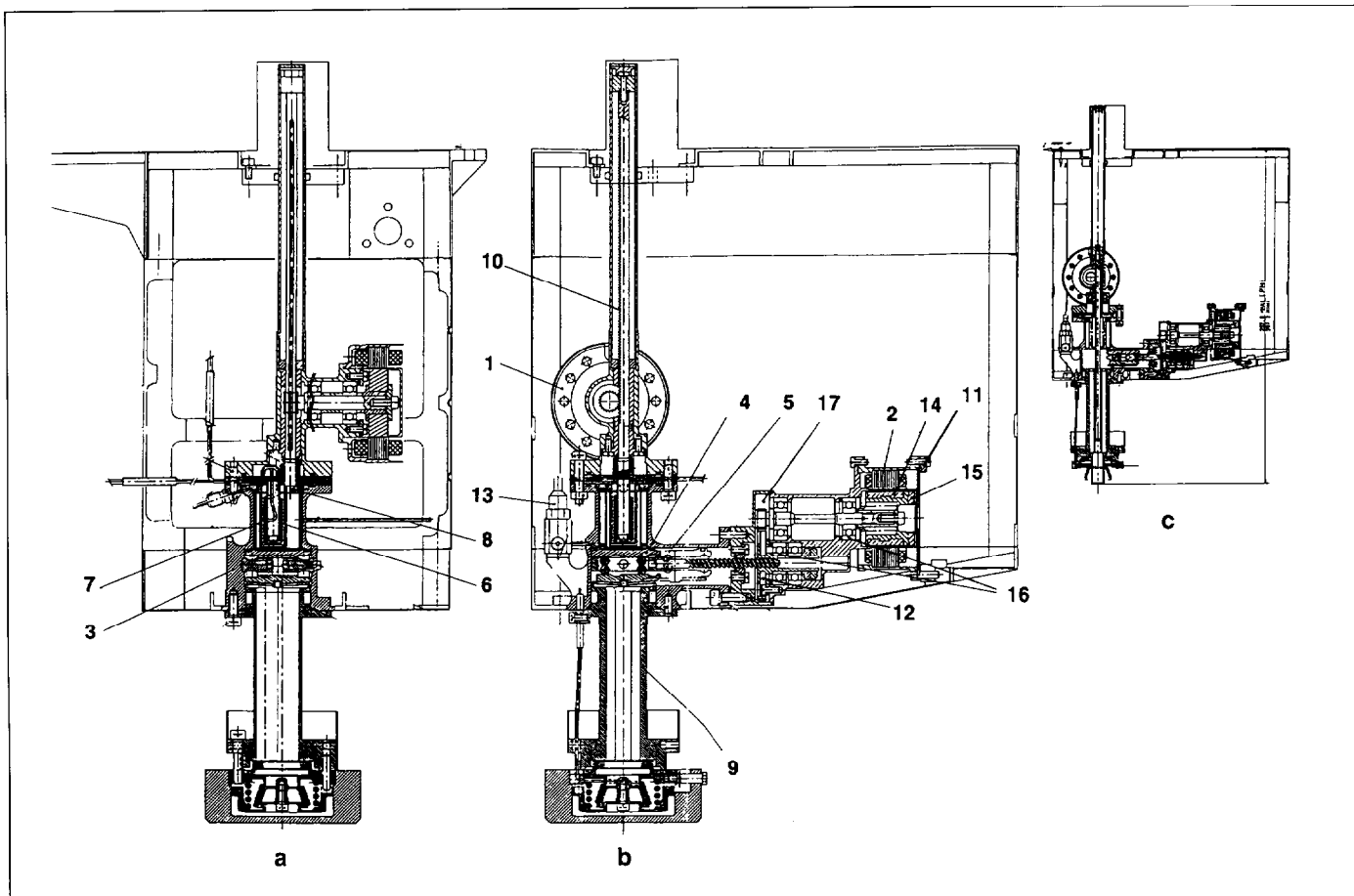
The filter is fixed at its base to a ring cramped to the filter mechanism rack, which moves it in and out of the oven. As shown in Fig. 6a, the filter's axis is displaced a few mm from the oven's main body axis. The penalty is a relative large dead volume. Taking into account the geometry of the three associated injection valves V1, V2, VT (see Section 3), the oven's dead volume totals 6 cm^3. In order to minimise chemical reactions with the walls, the oven body's inner surface body is gold-coated (few-μm layer).

The three injection valves are miniature solenoid valves made by Matra Marconi Space, procured with their Lee restrictor (Lee Jeva) mounted as shown in Fig. 8. They are monostable normally closed. Each is made of stainless steel with Viton elastomer seats to withstand very low temperatures ($-25°$C).

For transferring effluent gas and pyrolysis products to GCMS, the carrier gas is a labelled nitrogen $^{15}N_2$, to avoid unwanted secondary reactions with Titan's atmospheric nitrogen. The carrier gas is stored in a specially developed reservoir (GT) at 30 bar. The 55 cm^3 cylindrical gas reservoir has a 32 mm diameter and its housing is made of 1 mm-thick stainless steel. The system is designed for a maximum pressure of 40 bar at 120°C; burst pressure is 160 bar. The oven is supplied through the one-shot P3 valve, specially developed and qualified by Industria. This solenoid valve actuates a needle that punctures a metal diaphragm to initiate carrier gas flow. The diaphragm is a few μm thick and is qualified for the large pressure differential (upstream flow 40 bar, downstream 2 bar).

An identical one-shot valve is used for P1, which isolates the ACP gas transfer system from the PTL and GCMS inlet tubing (see Fig. 1). P1 was calibrated for identical pressures (3 bar) upstream and downstream.

7.2 Filter mechanism (FIM) and stepper motor

FIM and the GV mechanism were both designed by Mecanex (Switzerland), an SEP subcontractor. FIM is a rack and pinion mechanism that translates the filter 120 mm along ST between the sampling position and the oven inner position. A guide tube is used as a housing for the rack in its retracted position. Accurate translation of the stainless steel rack is by two bronze sliding bearings above and below the pinion. Inside the bottom bearing is a ceramic anti-rotation ball that moves in a groove machined in the rack. A cupro-beryllium helical spring comprising three quarters of a coil pushes the ball into the groove, creating a 1 N rack pre-load. Near the bottom of the rack, a collar crushes an elastomer (fluorosilicone) O-gasket when the filter is in its inner position, ensuring a tight fit between the oven and FIM. At the rack's other end, a magnet holds the rack accurately in a tight and stable position during sampling and heating. During sampling, the 10 N generated by the magnet's proximity to the bottom magnet frame, fixed to the guide tube, pushes the filter's mounting ring against metallic bellows. During heating and product transfers (and the high vibration periods of launch and Titan entry), the magnet and the top magnet frame generate 13-17 N to hold the filter ring contact against the oven base. Two Hall effect sensors (FHI and FHO) detect the filter end positions. A 22-tooth bronze spur gear, 8.8 mm pitch diameter and 3.6 mm wide, transmits the motor's rotary motion to the rack. Two ball bearings are assembled on the common pinion and motor shaft, pre-loaded to 6 N with a ring. Structural elements (the mechanism case, guide tube and top cap) and most of the fittings are made of titanium alloy.

SAGEM's 21 PP 61 electric stepper motor was selected for FIM. This 200-step motor provides a starting torque of 0.139 N.m and then a constant torque of 0.092 N.m. The drive unit monitors it with a square wave command of 6 ms per step. Each step rotates the motor shaft by 1.8°, translating the filter by 0.138 mm. Total time from one end position to the other is 5.250 s, in either direction.

7.3 The gate valve (GV) system

The GV system is composed mainly of the GV itself, the mechanism (GVM) and the motor (GM). A guillotine valve was preferred over a spherical valve, which required an excessive stroke for the filter. The specially developed device (SEP) allows the filer to translate in both directions. It must also ensure the oven's integrity for any pressure up to 3 bar. GV's main components (see Fig. 7) are:

1. the valve main body (common with the oven body), the roller plate, the top and bottom clappers, all made of stainless steel;
2. the rollers and the two springs (pre-load spring and return spring), made of cupro-beryllium.

The pre-load spring is an 8-point star, 1.2 mm thick and 28 mm wide. It is fixed against the lower clapper, with its extremities bearing on the top shoulder of the exaust tube. The return spring is located between the top and bottom clappers; it exerts a permanent force to maintain the clappers against the rollers. GV is in its minimum thickness configuration when the rollers are in two grooves machined on the clapper profile. The valve's closing stroke comprises two parts. The first, 23 mm along the GV screw axis, blocks filter access to the sampling tube (closing phase). The second part, 5 mm further along, brings GV against the bottom collar of the oven body (locking phase).

GV's closing and locking operations is as follows. First, the screw pushes the roller plate. Since the return spring exerts a 14 N restoring force on the top and bottom clappers, the clappers remain stuck against the rollers for minimum thickness and GV translates towards the closed position. When GV reaches this position (the extremity
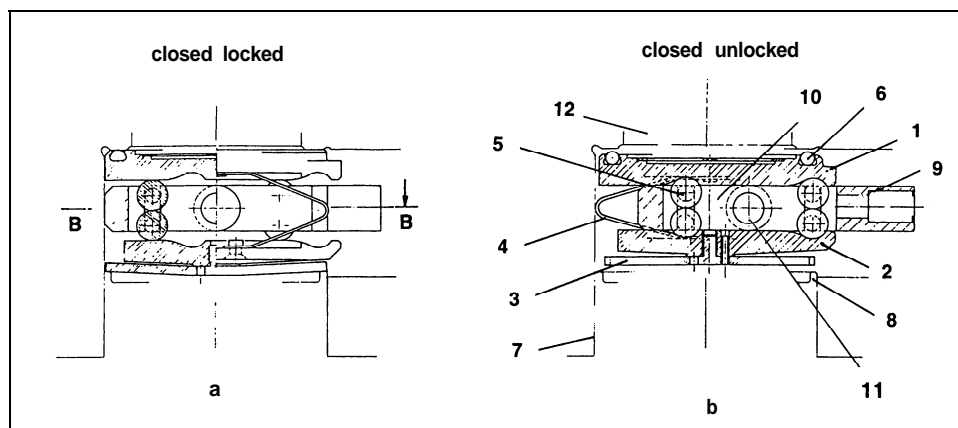
Fig. 7. Gate valve. 1: upper clapper. 2: lower clapper. 3: pre-load spring. 4: return spring. 5: roller. 6: O-ring gasket. 7. sampling tube (ST). 8: ST shoulder. 9: GV power arm. 10: roller plate. 11: guide. 12: oven.

of the clapper against the body), the screw pushes the roller plate and the rollers start to move outside their grooves. GV thickness increases until the roller plate is stopped by the valve's main body. At that point, an O-ring gasket with a groove machined into the top clapper is crushed between the oven collar and the clapper. The crushing force (387 N) is provided by the pre-load spring. GV is then in its locked (and gas tight) position. The groove profile is designed to provide the best transfer function between axial and vertical loads along all of the roller path. The O-ring gasket is made of fluorosilicone elastomer as tests have shown that a metallic gasket could not satisfy the high tightness requirement of 5×10^{-4} mbar.l.s^{-1}. A GV-mounted magnet provides the output signals of the Hall effect sensors: GVHC for closed and locked position, GVHO for open position (see Fig. 1). Duration of the complete operation 5 s.

GVM, which transforms the motor's angular motion into GV screw translation, comprises mainly the motor and its shaft, a spur gear, the GV power screw and the bearings. The stainless steel motor shaft, 66 mm long and 4 mm outer diameter, has two deep-groove bearings mounted on its shoulders. It transmits motor torque to the input pinion, which meshes with the wheel. The module ratio (pitch diameter divided by the number of teeth) and the speed reducing ratio of the gear have been chosen as 0.4 and 4, respectively. The input pinion's pitch diameter is 8 mm; hence the wheel's pitch diameter is 32 mm. The screw-and-nut stage consists of the GV power screw and the thread machined inside the wheel (which acts as a nut). The helix has a mean diameter of 3.4 mm, a pitch of 2 mm and a lead angle of 80°. The power screw translates within the wheel's hollow axis. Using a bronze-stainless steel combination
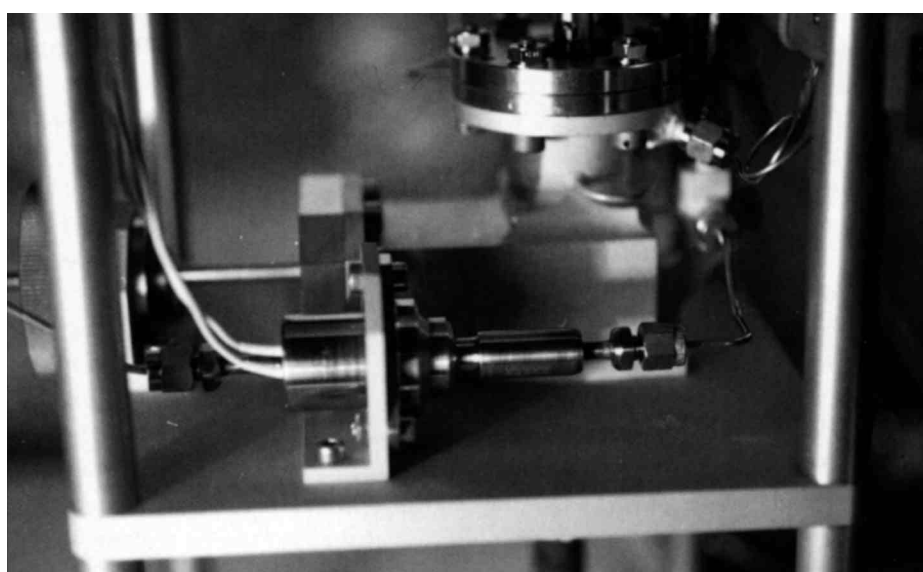

Fig. 8. The Matra Marconi Space electrovalve, with the Lee restrictor mounted on the right side.

avoids the need for lubricants: the input pinion and screw are made of stainless steel, while the wheel is of bronze. Although not shown in Fig. 6, three ball bearings are mounted on the wheel's axis, a thrust bearing on each side of the wheel and a deep-groove bearing at the end of the axis, on the opposite side of the GV. As for the filter mechanism, almost all of the structure and fitments are made of titanium alloy. Examples are the mechanism case, and the nut and counternut of the GV axis.

GVM is an ETEL Meti 111 brushless DC motor with two phases and five pole pairs. The 672 rpm rotation speed satisfies the 5 s requirement for the total stroke time. When supplied with a nominal power of 10 W, the motor provides the 115 mN-m torque for the total 250 N thrust needed for GV locking and friction compensation. Two Hall effect driving sensors, 36° apart, detect the pole positions and serve as input signals for the electronics drive unit that provides the motor with the proper square wave supply.

7.4 The bearings

Two bearing types are used for the filter mechanism and the gate valve mechanism: five deep-groove ball bearings (two for FIM and three for GVM, operated with a combination of radial and axial loads), and two thrust ball bearings (mounted on the wheel axis to compensate for pure thrust loads). Both types were manufactured by RMB (Switzerland). The deep-groove bearings have an outside diameter of 19 mm and a bore diameter of 5, 6 or 7 mm, according to the bearing location, with a total static load capacity of 300 N and dynamic load capacity of 600 N, providing a design margin >7.

Because of the requirements for very low chemical contamination inside ACP, the use of lubricants and organic materials was excluded as much as possible. Hence, for the deep-groove bearings, ceramic balls are used with stainless steel rings and the cages are covered with a sputtered silver layer. The two thrust bearings are identical devices, with 19 mm outside diameter and 8 mm bore diameter. They are specified for a static thrust capacity of 2200 N and a dynamic thrust capacity of 1300 N; ceramic balls are used with chrome steel rings and brass cages. Pre-load computations showed that all the bearings need a 6 N pre-load except those on the wheel axis, where it is limited to 3 N to avoid excessive friction torque on them.

8. The Sampling System

Owing to the high temperatures required for pyrolysing the organic compounds, the use of metallic mesh filters with fibres of a few μm diameter was necessary for collecting the aerosols (see Section 7). It was thus imperative to test the behaviour of these materials under ACP experimental conditions. Tests were performed in low pressure chambers (at SA/CNRS and CNES) to evaluate the pressure drop produced by such metallic filters as the pump unit draws in Titan's atmosphere. Using the cold gas test facility of CERT/ONERA in Toulouse (see below), it was possible to study the effect of low temperatures. The theoretical laws giving the variation of the pressure drop with temperature and total pressure (Fuchs, 1964; Pich, 1971) were verified and used to characterise the pump.

It was also necessary to evaluate the collection efficiency for sub-μm particles when metallic filters operate at reduced pressure. The tests were performed at the Institut de Protection et de Sûreté Nucléaire/CEA, Saclay, using Na-Fluoresceine (Uranine) particles 0.15 μm in diameter. Such a particle size corresponds to the lowest efficiency of a fibre filter. For larger sizes, the impaction of particles inside the filter increases the efficiency (Suneja & Lee, 1974); for smaller sizes, capture due to brownian diffusion predominates (Davies, 1952). These tests led to the choice of multi-layered Beckeart ST10 filters (porosity 80%, thickness ≈ 0.4 mm, fibre diameter ≈ 0.4 mm),

which provide the best trade-off between efficiency and pressure drop for our experimental needs.

Aerosols are collected by direct impaction during the first sampling phase (135-80 km). The pump unit draws atmospheric gas through the filter during the two aerosol sampling periods at 80-32.5 km and 22-17 km nominal altitudes. A kinetic wheel design was selected - a 19 000-25 000 rpm drag fan.

8.1 Description of the pump

The pump (Fig. 9), built by Technofan under subcontract to SEP, is a small, light-weight unit of about 850 g and overall size 100x80x100 mm. The system consists of
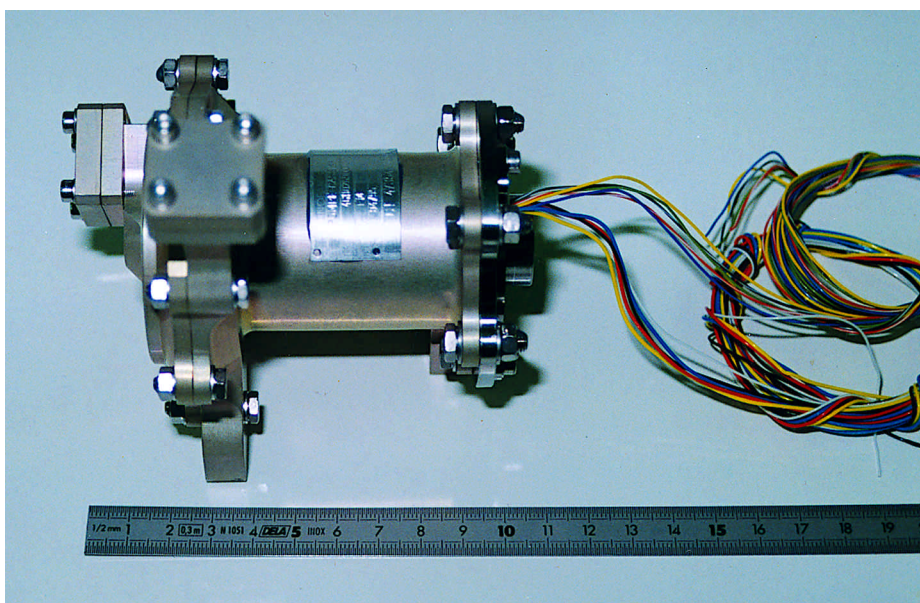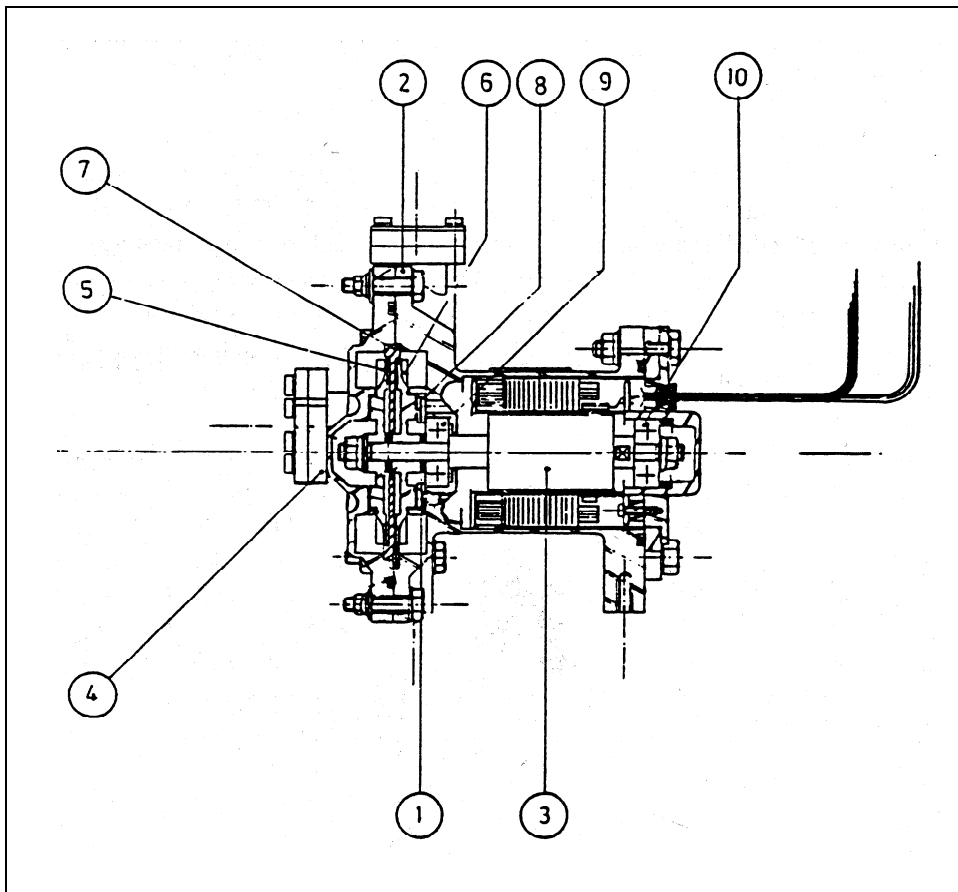
Fig. 9. The pump unit. 1: titanium spacer. 2: second stage volute. 3: rotor. 4: first stage volute. 5: first wheel. 6: second wheel. 7: sealing plate. 8: front ball bearing plate. 9: front ball bearing. 10: read bearing.

a casing, the first/second stage pump wheels and the electric motor. The internal assembly is mounted on a shaft carried on two bearings. The first and second stage pump wheels are mounted on the motor shaft and locked to the inner race of the front bearing by the shaft lock nut. The front bearing is mounted in a housing, integral with the casing, restraining the bearing outer race from axial and radial movement.

At the rear end of the pump, a rear bearing is held in an adjustable cover. Radial movement is restrained but axial movement is limited only by the pre-load from a compressive washer giving about 40 N around the outer race. As the dynamic mass of the shaft assembly is of the order of 125 g, the 40 N pre-load is sufficient to prevent axial movement up to 33 g applied axially to the shaft dynamic mass. The shaft is not free to move axially because it is restrained by the front end bearing housing and the bearing axial stiffness. The pre-load ensures that the axial and radial play in the bearings is taken up, allowing for greater stiffnesses against radial or axial movement. The shaft assembly is completed by a second locknut that pre-loads the rear bearing inner race. The shaft and its bushes and abutments are of good quality stainless steel. The electric motor rotor is fixed in the middle of the shaft in the correct position with respect to the stator winding. The radial clearance between rotor and stator is only 0.3 mm. The winding is fixed permanently to the motor casing, which is purely cylindrical at this section. A titanium sleeve around the stator protects the internal parts of the pump (and sampling tubing) against chemical contamination.

At the pump front end, formed around the circumference of the motor cylindrical casing, is a housing to accommodate the front cover. The two form the first and second stage pumping cavities. Eight stainless steel bolts attach the front cover to the housing. The front housing also provides the load path down to the two front attachment legs, which are equispaced around the shaft axis. Only one rear attachment leg is provided, and this is accommodated by the rear housing, which has a similar function to the front one in that it accepts a cover. Six bolts are used for the rear cover attachment. The front cover, front housing, cylindrical casing, rear housing and rear cover are all made of aluminium. In order to achieve the leak rate requirement (10^{-7} mbar.l.s^{-1}) Viton seals were preferred to metal seals.

The motor is a brushless (permanent magnet) 3-phase auto synchronous motor from Norcroft. Hall effect sensors monitor the rotor position. The maximum electric power required for the pump is 69 W. The two bearings, mounted on the pump shaft, are deep-groove ball bearings. A high rotation speed (above 25 000 rpm), no lubricant and a 10 h lifetime are the strong constraints the bearings have to satisfy. Ball bearings pre-loaded to 36 N with stainless steel rings and balls, and a cupro-berylium cage were envisaged, but development tests showed there was material transfer between rotating parts, thus jamming the bearings after few seconds' operation at high speed. The bearings finally selected use stainless steel balls and rings, and a DUROID 5813M cage. The DUROID is a glass microfibre PTFE with MoS_2 as an additive. In use, the MoS_2 coats the balls, forming a dry lubricant.

As for the filter and the gate valve mechanisms, the bearings were manufactured by RMB and have an outer diameter of 19 mm. Moreover, this choice allowed the pre-load to be reduced to 6 N. Tests were performed for >40 h at 25 000 rpm, highlighting the system's good behaviour: the average torque remained below 20 g.cm for almost the whole test duration.

8.2 Aeraulic tests under Titan atmospheric conditions

Aeraulic tests were conducted on the pump unit by using the Cold Gas Test System developed by ONERA at Centre d'Etudes et de Recherches de Toulouse (CERT). The system shown in Fig. 10 was developed under ONERA's contribution to the ACP programme for filter sampling characterisation. The test objective was to analyse the pump's air flow performance when inlet temperature and pressure are close to the values expected during Titan descent.
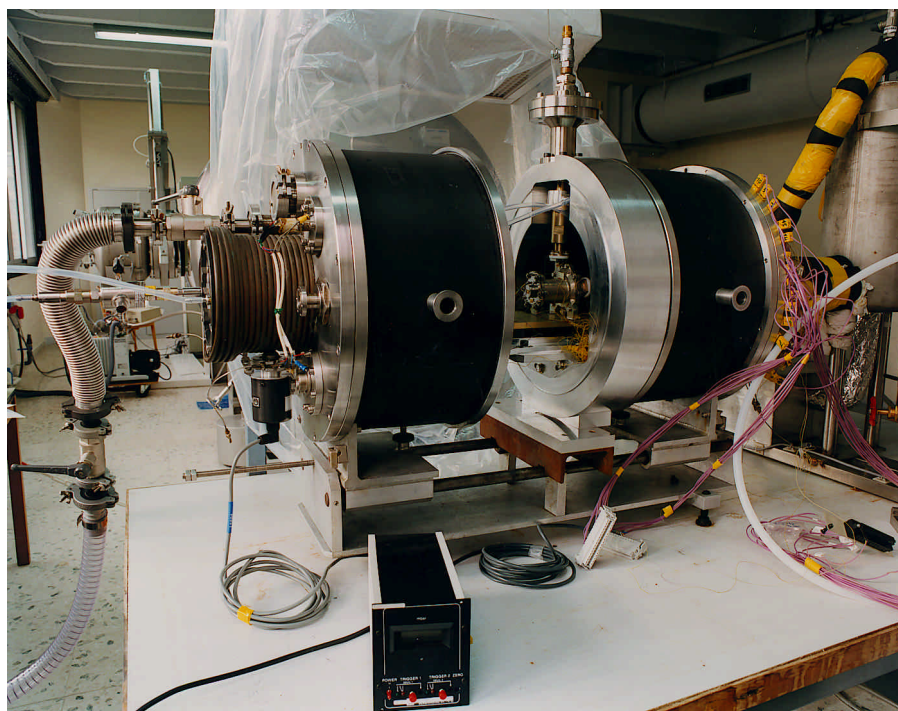
CERT's Cold Gas Test System consists of:

1. the cold gas generator - a liquid nitrogen reservoir, a cryogenic valve controlling liquid nitrogen flow, and a heat exchanger of a coiled pipe immersed in the liquid flow stream;

2. the test chamber of two 55 mm-diameter double-wall cylinders and two internal pipes to carry refrigerant fluid. The two movable cylinders are separated by a central flange;

3. an interface flange that connects the cold gas generator to the test chamber. The flange is screwed to an inlet cylinder fixed to the chamber and cooled by a liquid nitrogen helical pipe;

4. the accessory equipment - vacuum pump units, mechanical valves and electro-valves, and sensors (flow rate meter, pressure and temperature).

The test chamber can accommodate a large range of mass flow rates (20-200 mg/s) and of atmospheric pressure (from atmospheric pressure down to 30 mbar). Inside the chamber, the gas temperature at the exit tubing of the cold gas generator depends on the pressure (and Probe altitude) being simulated. Three altitudes were selected for the pump aeraulic tests: 65, 40 and 22 km; the exit temperatures were -100, -150 and -170°C respectively. Fig. 11 shows the system as used for the CERT tests. The results on the pump's air flow performance were compared with the pump's calculated dynamic characteristics. They were also compared with the results of aeraulic tests done by Technofan on their laboratory bench (at 25°C). In this case, the tests were for specific parameters (mainly pressure inlet) calculated to reproduce flow conditions with a Reynolds Number identical to that calculated from ACP's operating conditions.

Also, during the CERT tests, temperature sensors were located in different parts of the pump housing and support. The results have validated the thermal modelling of the pump made by Technofan.

8.3 Analysis of the microvibrations

As a result of the pump's dynamic characteristics (19 000-26 000 rpm, rotating mass 110 g, total unbalance 10 mg), it was decided to investigate the type of vibrations generated by the pump. Specific tests were performed at CNES with the pump mounted on a representative model of ACP. The tests pointed out: (1) under steady state
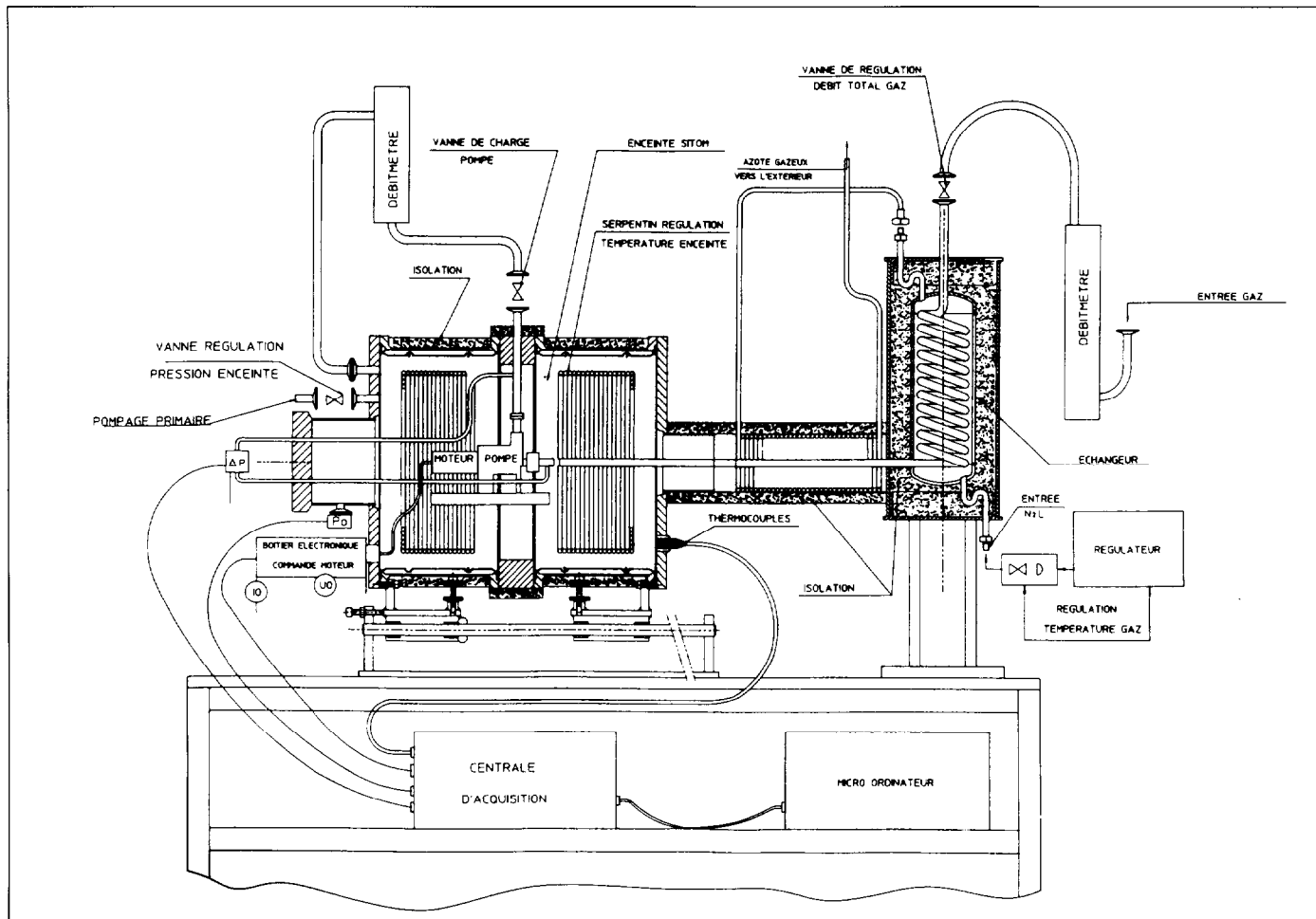
Fig. 11. Schematic of the bench test for pump flow characterisation.

conditions, there is a maximum force of < 11 N in both directions of the rotation plane at 23 200 rpm; (2) very brief peaks (59 N maximum) in the same directions during the transient starting and stopping phases (10 s). It was shown during integrated system tests at the Probe level that there was no incompatibility with the operation of the other instruments.

9. Electronic System

9.1 Hardware design

ACP's electronic system (ACPE) is composed of four functional blocks: DC/DC converter, control unit, monitoring unit and drive unit. The structure has two frames and a base plate, both made of aluminium alloy (Fig. 12). The first frame contains two parallel printed circuit boards (PCBs), one for the control unit (ACPCU) and one for the drive unit (ACPDU). The second frame, which has an integrated top plate, contains the monitoring unit (ACPMU) PCB and the components for the DC/DC converter block (Fig. 13a). After final integration the two frames are screwed together; the base plate is attached to the first frame, interfacing with the ACP mechanical main box (see Fig. 5).

Huygens supplies ACP with three 28 V power lines: main lines ML1 and ML3 and protected line PL2. ACPDC's main functions are: (1) to provide ML1 input with DC conversion for supplying other electronics functional blocks; and (2) to provide all power lines with EMI filters. Conversion of ML1 DC is performed through a circuit that uses in series an SAE, AFC 461 F/CH for transient suppression, an SAE AT 02815
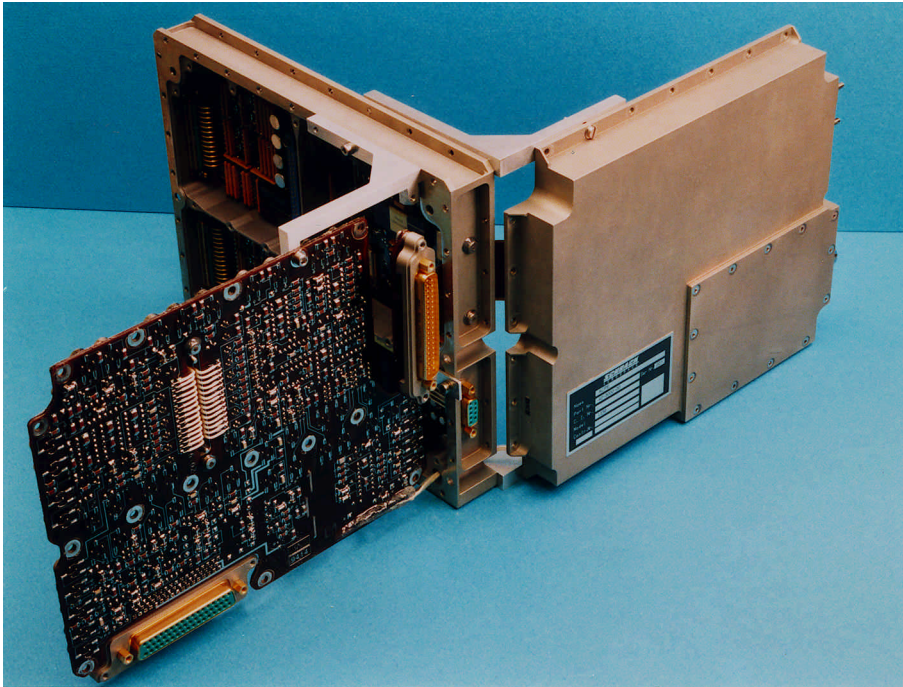
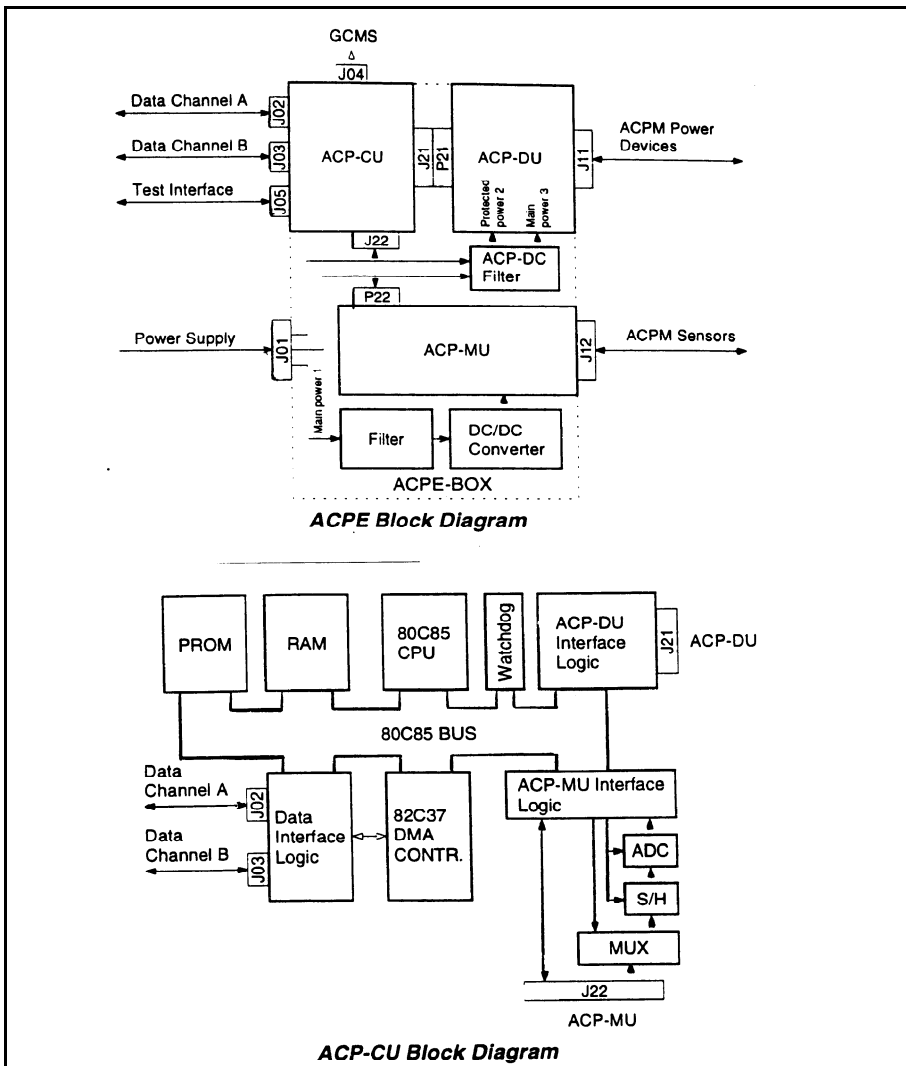**Fig. 12. ACP's electronics box.**

**Fig. 13. Top: the ACPE electronics block.
Bottom: the ACPCU control unit block.**

TF/CH for DC/DC conversion and one specific EMI filter to each output of the converter (0, +5, -15, +15 V).

ACPDU (Fig. 14) drives all the electromechanical devices (electrovalves, heaters, motors) of the mechanical box. DU is galvanically isolated from the drive logic in CU. ACPMU conditions and monitors the temperature and pressure analogue signals coming from the sensors in the mechanical main box. Under software instruction, ACPCU controls ACP's motors, valves and heaters (Figs. 13a and 13b); For that purpose, it monitors first, inside ACPE, the transfer of actuation commands to ACPDU the flow of digital and analogue inputs from ACPMU. It also monitors all data transfers and synchronisation with ACP external systems such as the Probe, GCMS and ACP's EGSE.

The data are transferred in two directions: (1) from the Probe's Command and Data Management Subsystem (CDMS) to ACP - mainly telecommands, descent data broadcast (DDB) and broadcast pulse (BCP); and (2) from ACP to the Probe - statusword and packet telemetry data (PTD). Synchronisation pulses are sent to GCMS for accurate timing of GCMS and ACP valve actuations during transfer periods. For activating and controlling mechanical and pneumatic components, the command signals generated within ACPCU are sent to ACPDU through a J21 connector. Status and sensor readings from ACP elements are transferred, after conditioning, to ACPMU.

ACPCU's main components are the 80C85 8-bit microprocessor, the 80C37 direct memory address (DMA), a 4.096 MHz oscillator, two PROMs with 8 kbyte memory each, two RAMs with 8 kbyte memory each, a 12-bit analogue to digital converter (ADC) with a sample and hold amplifier (S&H), two 8-channel multiplexers (MUX) and two FPGAs (field programmable gate arrays). In addition, ACPCU contains memory latches, buffers and optocouplers.

The microprocessor uses eight bits for data lines and 16 bits for address lines, eight of which are multiplexed with the address bus. The 4.096 MHz oscillator frequency is divided by one of the FPGAs to provide the non-maskable microprocessor interrupt with selectable clock pulses of 1, 2, 4, 8 or 16 ms. Two other interrupts of the 80C85 are used for BCP pulses every 125 ms (synchronised with the Probe) and overpressure
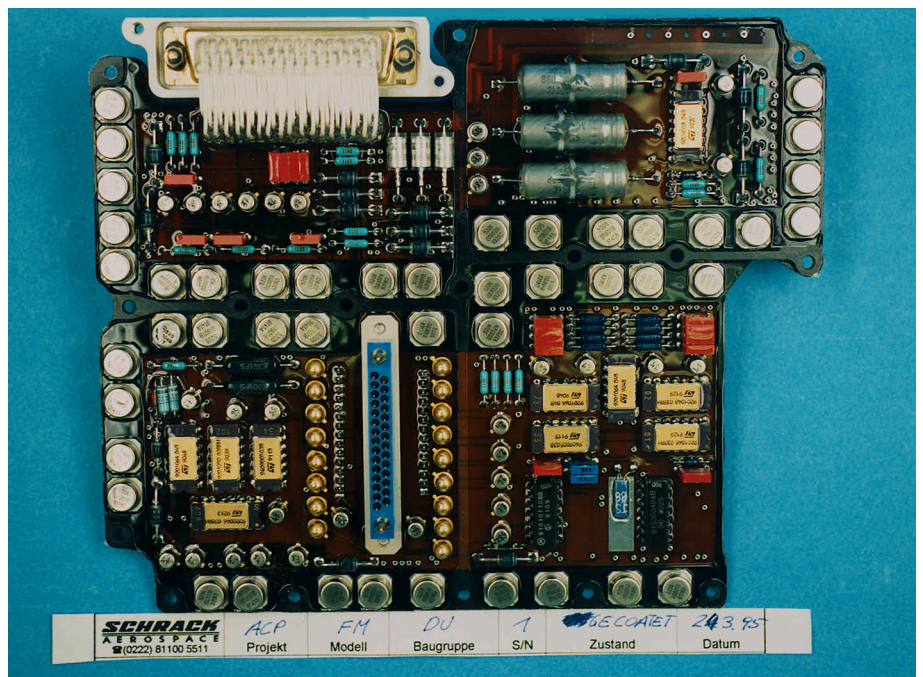

Fig. 14. The ACPDU electronics drive unit.

signals. The 12 kbyte program is stored in the two 8 kbyte PROMs. When the ACPE main line (ML1) is powered by the Probe, the 12 kbyte are transferred to the two 8 kbyte RAMs. The remaining 4 kbyte in the RAM serve as data transient memory.

DMA, driven by the FPGA timer, is used mainly for fast telemetry (TM) and telecommand (TC) management. Three of DMA's four request inputs are used for TM/TC data transfer from the 4 kbyte of the RAM to the Probe CDMS. The first two are used for nominal and redundant TM transfer, and the third for TC transfer.

The monitoring signals (temperature, pressure and status) coming from ACPMU are used by the software for controlling the instrument. Analogue signals (temperature and pressure) are multiplexed and converted to digital signals into ACPCU. A total of 15 analogue input lines is multiplexed through the two MUXs. The MUXs output line selection is performed by one FPGA, then the selected signal is transferred via the S&H to the ADC for analogue to digital convertion.

One of the two FPGAs controls the exchange of signals with the Probe (BCP, DDB, TC, TM). It also serves as pump current and speed counter. The other FPGA provides the microprocessor with a timer and a watchdog, and manages the ACPCU and ACPMU multiplexers. This FPGA also controls all the output command signals to ACPDU.

9.2 Software design

Onboard software is used by ACP's microcontroller to execute the automatic sequences, monitor the status and health of the various subsystems, acquire and interpret TC and format data for TM. Its main functions are to control the mechanical subsystem, collect data and transmit it to the Probe system, provide an interface to command ACP via the Probe, and perform descent measurements synchronised with the rest of the Probe.

ACP's software provides four different operational modes: descent; cruise checkout; ground test mode; engineering mode. The first three execute automatically on receipt of the appropriate mission flag and time. The engineering mode is selectable by a specific TC, and is used mainly for integration and test phases. In this mode, all ACP functions can be activated individually by sending the appropriate TC. It is accessible during any automatic sequence. It can also be used to check specified mechanical devices during cruise should any problem arise.

10. Science Validation and Calibration Test

10.1 Pyrolysis tests

In order to validate ACP's scientific performance, pyrolysis tests were conducted at LISA in Paris on solid phase material synthesised from experimental simulation. The organic synthesis by electrical irradiation of an N_2-CH_4 mixture requires a long reaction time (about 20 h). The reactor is a two-part glass vessel with two tungsten electrodes and a metallic filter in the lower part. It is filled to a total pressure of 900 mbar with a mixture of N_2 (800 mbar) and CH_4 (100 mbar). One of the electrodes is connected to a Tesla coil fed by a low current (80-100 mA) high frequency (80-200 kHz) generator. The other electrode is Earthed. Five irradiation periods of about 4 h each were performed and, between each, the gas phase was removed from the reactor and replaced by a new mixture of N_2-CH_4 at 900 mbar with the same ratio as the original. During irradiation, the bottom of the reactor was cooled by liquid nitrogen. At the end of the synthesis, 2.3 mg of solids were deposited on the filter.

An ACP model (M3) was specifically developed for this sort of science validation and laboratory investigation (see Fig. 15). It is representative of ACP except for the pump unit and the gas tank, which are not mounted. However, it contains:
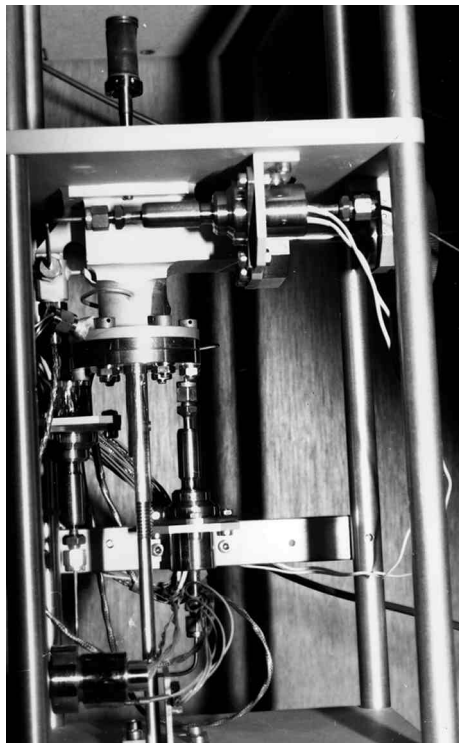
Fig. 15. The M3 model mounted on the calibration bench at LISA.

– the filter transfer mechanism (not motorised) to translate the filter into and out of the oven;

– the gate valve mechanism (not motorised) to close off the oven;

– the three monostable microvalves used to vent the oven by pumping (VT) to fill the oven with pure nitrogen piston gas (Vl), and to transfer the gas phase from the oven to GCMS (V2).

The filter could be dismounted from its support and easily replaced. In order to protect the filter's organic solid phase material from oxygen contamination, the following operations were carried out in a glove box filled with nitrogen:

– once removed from the reactor, the filter was mounted in M3;

– M3's gate valve was closed after enclosing the filter in the oven.

Owing to the oven's low leak rate ($<10^{-3}$ mbar.1.s^{-1}), we can be sure that no oxygen contamination of the filter occurred during analysis. The analysis of the pyrolysis products was done at LISA, where a Varian Saturn II GCMS was used (with helium as carrier gas) at an inlet pressure of 1.6 bar. The chromatographic capillary column was a CP-Sil-5 CB column of 25 m length, 0.15 mm inside diameter and 1.20 mm film thickness from Chrompack. The column temperature was controlled thus: 30°C for 20 min; raised from 30°C to 150°C in 30 min at 4.0°C/min; 150°C for 10 min. The total mass spectra of the GC peaks were thus collected over 60 min. The ion trap detector was able to detect masses of 10-226 amu by using the electronic ionisation mode. The experimental chromatographic conditions were chosen to detect hydrocarbons from C_4 to C_{10}, which excludes any information about the light hydrocarbons (C_2 and C_3) and the heavy hydrocarbons (above C_{10}). Using this experimental approach, we achieved a very good validation of ACP for the 600°C pyrolysis sequence that will be performed on the sampled aerosols during Probe descent.

The chromatogram obtained by GCMS analysis of the synthesised solid phase yields a pyrogram showing many organic compounds (Figs. 16a and 16b). Some GC peaks appear clearly from the total mass spectra. The others are identified only when they are specific ions with a very high MS sensitivity. According to their mass spectra, 23 gross formulas of more than 25 GC peaks have been identified unambiguously. The numbered peaks (Fig. 16) were identified and the possible isomers according to their mass spectra were suggested. It immediately appears that no. oxygenated organic compounds were detected, showing that the laboratory procedure prevented oxygen contamination of the synthesised solid phase material.

The main compounds detected on the pyrogram are mono aromatic hydrocarbons. The most concentrated is benzene (12), followed by toluene (16) and Q-substituted benzene (19, 21, 22). One may conclude that these mono aromatic hydrocarbons are the major constituents of the synthesised solid phase material. If they are thermally stable, they could be completely desorbed into the gas phase at 600°C with no variation of their structures. Thus the main constituents are the main compounds desorbed and detected on the pyrogram.

One argument limits the validity of this result. Since a bi-aromatic hydrocarbon is observed on the pyrogram (23) and because of the chromatographic conditions (choice of column), we cannot properly observe poly aromatic hydrocarbons. In a previous study, pyrolysis of anthracene, which contains three aromatic cycles, was performed with the same pyrolyser at 600ºC. The pyrogram showed mainly benzene, toluene, ethenyl-benzene and C_8H_{10} isomers. It shows that poly aromatic hydrocarbons are decomposed at 600°C in benzene and in substituted mono aromatic hydrocarbons. The type of compounds detected on anthracene pyrograms depends on the pyrolysis
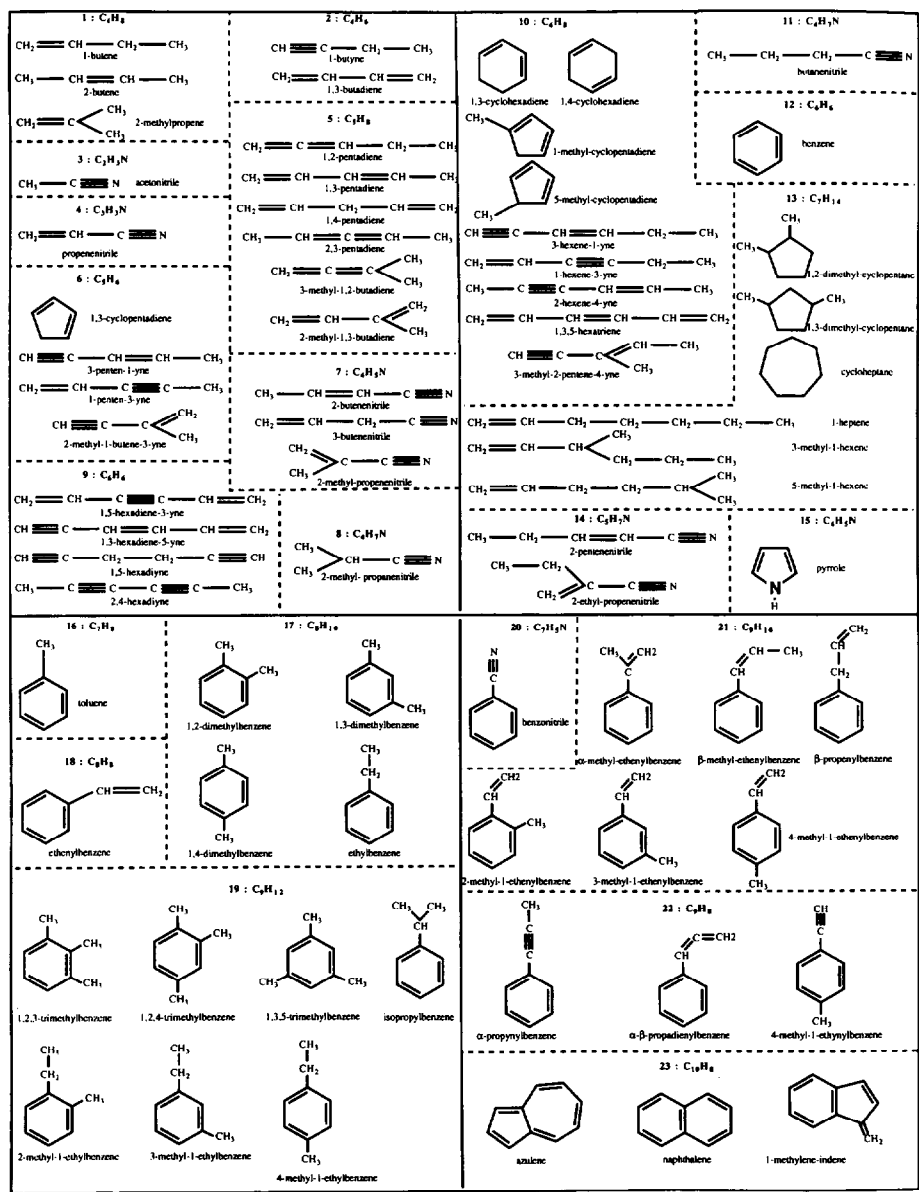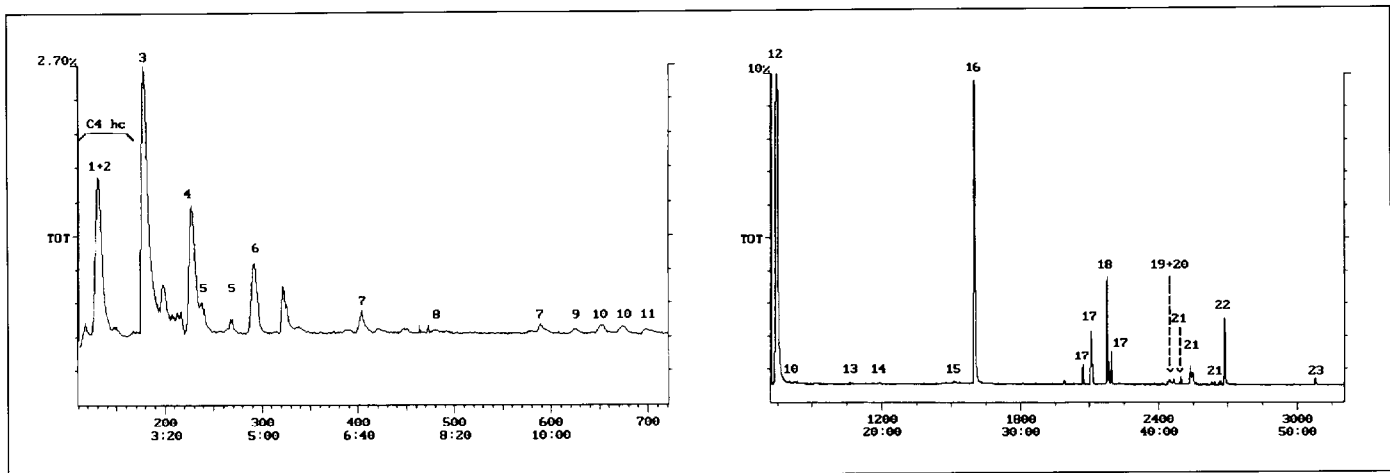
Fig. 16. Pyrogram of the solid phase material synthesised directly on to the M3 filter (above) and analysis (left).

temperature. For example, it was shown that naphthalene (a bi-aromatic hydrocarbon) was clearly observed at a lower pyrolysis temperature. So it is quite possible that the mono aromatic hydrocarbons detected on the pyrogram could be provided by the poly aromatic hydrocarbons present in the solid phase material and thermally decomposed at 600°C into mono aromatic hydrocarbons.

We also detect a small amount of benzonitrile (20), which can be similarly produced by thermal decomposition of poly aromatic compounds containing nitrogen atoms. Most of the nitriles observed on the pyrogram have also been detected in the gas phase synthesised by the simulation (3, 4, 7, 8 and 11). The heaviest nitriles detected (14 and 15) could be provided by thermal desorption of the same compounds present in the solid phase or by thermal decomposition of the heaviest molecules. Finally, many hydrocarbons are detected on the pyrogram (1, 2, 5, 6, 9, 10 and 13). They can be provided by the two sources cited above, or by the thermal polymerisation of the lightest alkenes and alkynes.

Before performing the above pyrolysis tests, the procedure for testing the cleanliness of the ACP Flight Model, after delivery by SEP, was conducted on M3. The instrumentation includes a very pure nitrogen gas reservoir, a flow regulator provided by the contractor, and laboratory GCMS. A mixing ratio threshold of 50 ppb was measured for the significant gas components.

10.2 Validation tests of the direct Mass Spectrometer mode

Tests were run to verify the ACP transfer cycle described in Section 5 and to validate the data obtained by GCMS in the direct MS mode (direct inlet flow into the dedicated ACP ion source of GCMS). Several nominal sequences reproducing the ACP transfer cycle were conducted at LISA using a commercial quadrupole mass spectrometer. The verified transfers correspond to the nominal descent phase when ambient oven temperature analyses are made after the first aerosol sampling period. GCMS valve VAB was replaced by a commercial Bürkert valve to which a commercial Lee-Jeva restrictor, representing FRA, was added (see Fig. 3). Flow restriction equivalent to that provided by VL4 on Huygens was reproduced by using a capillary fused silica tubing of 10 μm internal diameter and 6 cm length. Fig. 17a gives the curve of peak mass 28, which is representative of the evolution of the pressure (nitrogen) in the V2-VAB line, following the 8-pulse cycle (see Fig. 4). For testing the ACP-MS coupling, the oven was filled at 30 mbar with pure krypton. The mass spectra obtained (mass 84, Fig. 17b) is representative of the amount of krypton injected. Quantitively, the decrease in krypton's pressure corresponds exactly to the specifications for transferring the oven's atmospheric content. It confirms that the calibration of the FRA restrictor used for the M3 model (Lee Jeva 80000 Lohm) gives the correct flow for the ACP-GCMS coupling of the Huygens experiment.

The observed pressure peaks correspond to the simultaneous opening of V2 and VAB causing an increase in the total pressure and krypton's partial pressure in the V2-VAB line. This phenomena is smoothed on the figure by acquiring one point per second. In the GCMS experiment, a scan of the entire mass spectra will last about 2 s, so the smoothing of the curve obtained should be greater.

10.3 The calibration programme

The programme selected for calibrating the flight models is directly linked to the GCMS calibration plan (see the GCMS paper in this volume). As GCMS will analyse the gas products transferred from ACP, the calibration system at NASA Goddard was used to relate (qualitatively and quantitively) GCMS' mass spectra to the effluent gases injected from ACP. ACP calibration is a 2-step process and concerns only the gas phase transfer. This is because we do not wish to pollute the Flight Models' ACP internal tubing and GCMS analyser with products of solid samples such as tholins or

other complex matter. The tests allowed the evaluation of GCMS' response to the ACP products.

The first step directly injected several calibrated gas or gas mixtures containing expected Titan ratios into the ACP feed tube (IVA-VAB in Fig. 3). The second step, which requires the calibration gas to pass through ACP first, has been delayed because of the very tight GCMS delivery schedule. This part of the calibration programme will be performed immediately after launch, on the two spare models.

The second step was similar but the calibrated gas passed through ACP first. For that, the calibrated gas mixtures were injected from Goddard's calibration bench into the oven using the special inlet T3 (to be pinched off, see Fig. 1). During the investigation, the oven will be heated according to ACP's timeline before each nominal
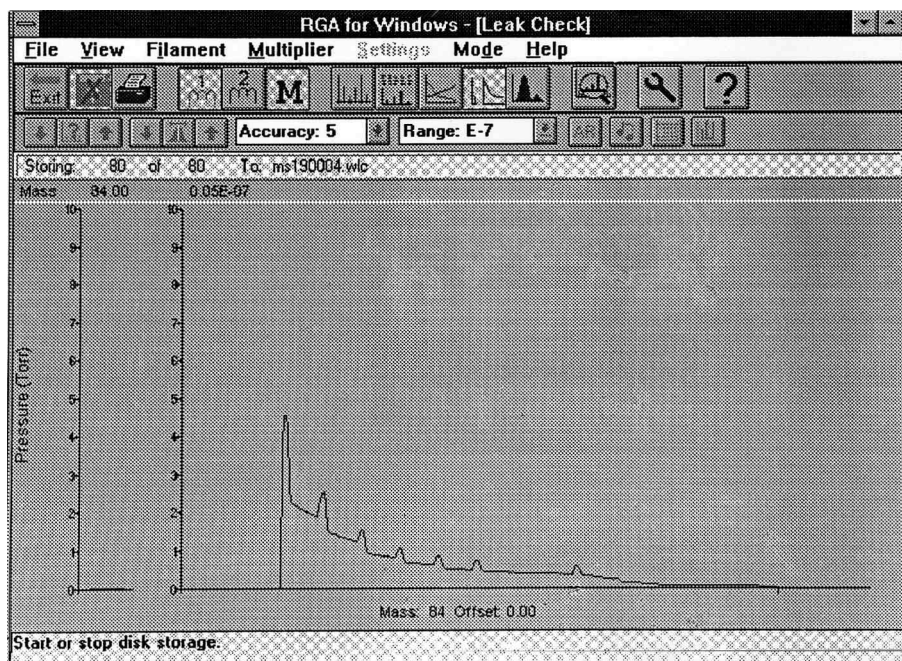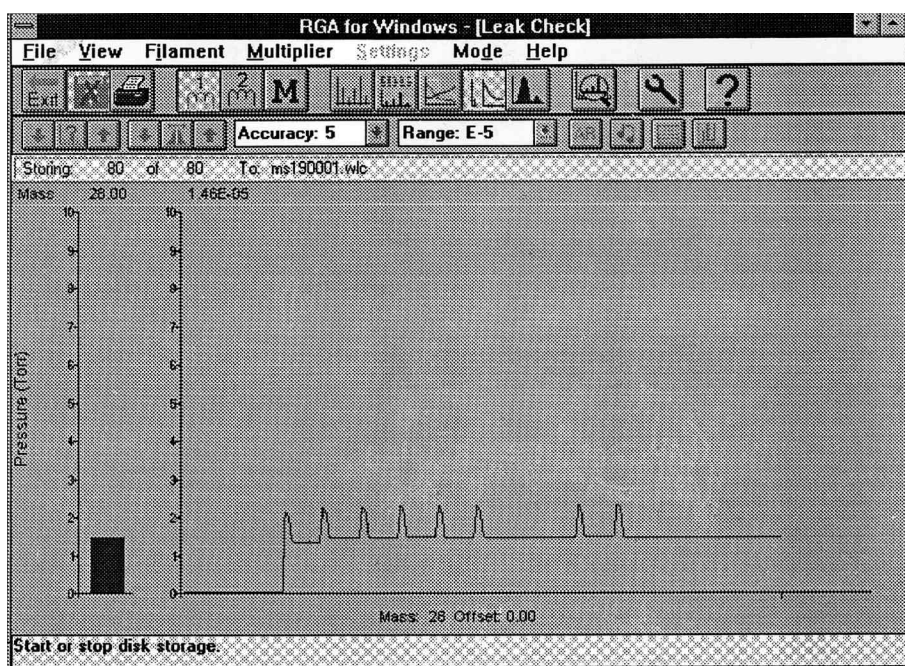

Fig. 17. Validation of the transfer cycle by using the direct Mass Spectrometer mode. Top: N$_2$ pressure evolution during injections. Bottom: gas sample (Kr) peak variation during transfer.

transfer cycle. The oven pressure will be set to simulate the conditions after the completion of each of the two aerosol sampling phases. The oven's gas tightness when the gate valve is locked is sufficient (leak rate 10^{-3} mbar.l.s^{-1}) to prevent any change in the calibrated gas concentrations during the analysis process.

In the ACP configuration at Goddard, isolation valve P1 will be replaced by a dummy valve with a punctured diaphragm in order to allow passage through to GCMS. During ACP integration on Huygens, the pneumatic connection to GCMS was made by attaching PTL between the two. This was followed by a special procedure for cleaning and filling the PTL with pure N_2.

Flight Model cleanliness was assured and controlled by following the same procedure as with the M3 model. During post-launch calibration, pyrolysis tests and chromatographic analysis are planned at Goddard using representative mock-ups of the GCMS and ACP Flight Models.

References

Cabane, M., Rannou, P., Chassefière, E. & Israel, G. (1993). Fractal aggregates in Titan's atmosphere. *Planet. Space Sci.* **41**, 257-267.

Chassefière, E. & Cabane, M. (1995). Two formation regions for Titan's hazes: indirect clues and possible synthesis mechanisms. *Planet. Space Sci.* **43**, 91-103.

Davies, C. N. (1952). The separation of airborne dust and mist particles. *Proc. Inst. Mech. Eng.* **1B**, 185-198.

Ehrenfreund, P., Boon, J. J., Commandeur, J., Sagan, C., Thompson, W. R. & Khare, B. (1995). Analytical pyrolysis experiments of Titan aerosol analogues in preparation for the Cassini Huygens mission. *Adv. in Space Res.* **15**, (3), 335-342.

Frère, C., Raulin, F., Israel, G. & Cabane, M. (1990). Microphysical modelling of Titan's atmosphere, application to the in-situ analysis. *Adv. in Space Res.* **1**, 159-163.

Fuchs, N. (1964). *Mechanics of aerosols.* Pergamon, Elmsford, New York, USA.

Israel, G., Cabane, M., Raulin, F., Chassefière, E. & Boon, J. J. (1991). Aerosols in Titan's atmosphere: models, sampling techniques and chemical analysis. *Ann. Geoph.* **9**, 1-13.

Lebreton, J.-P. & Matson, D. L. (1997). The Huygens Probe: Science, Payload and Mission Overview, ESA SP-1177 (this volume).

Pich, J. (1971). Pressure characteristics of fibrous aerosol filters. *J. of Colloid and Interface Science* **37**, 912-917.

Rannou, P., Cabane, M. & Chassefière, E. (1993). Growth of aerosols in Titan's atmosphere and related time scales: a stochastic approach. *Geophys. Res. Letters* **20**, 967-970.

Raulin, F., Frére, C., Paillous, P., de Vanssay, E., Do, L. & Khlifi, M. (1992). Titan and exobiological aspects of the Cassini-Huygens mission. *J. of the British Interplan. Soc.* **45**, 257-271.

Suneja, S. K. & Lee, C. H. (1974). Aerosol filtration by fibrous filters at intermediate Reynolds numbers. *Atmospheric Environment* **8**, 1081-1084.

Toon, O. B., McKay, C. P., Griffith, C. A. & Turco, R. P. (1992). A physical model of Titan's aerosols. *Icarus* **95**, 24-53.

West, R. A. & Smith, P. H. (1991). Evidence for aggregate particles in the atmospheres of Titan and Jupiter. *Icarus* **90**, 330-333.